

1 **Title: Temporal coordination of collective migration and lumen formation by**
2 **antagonism between two nuclear receptors**

3

4 Xianping Wang¹, Heng Wang^{1*}, Lin Liu¹, Sheng Li², Gregory Emery³, Jiong Chen^{1*}

5

6 ¹ State Key Laboratory of Pharmaceutical Biotechnology and MOE Key Laboratory of
7 Model Animals for Disease Study, Model Animal Research Center, Nanjing
8 University, Nanjing, China 210061

9 ² Guangzhou Key Laboratory of Insect Development Regulation and Application
10 Research, Institute of Insect Sciences and School of Life Sciences, South China
11 Normal University, Guangzhou, China, 510631

12 ³ Institute for Research in Immunology and Cancer (IRIC) and Department of
13 Pathology and Cell Biology, Faculty of Medicine, Université de Montréal, Montréal,
14 QC Canada

15 * Correspondence: wangheng@nicemice.cn; chenjiong@nju.edu.cn;

16

17 Lead contact: Jiong Chen (chenjiong@nju.edu.cn)

18

19 **Keywords: E75; DHR3; nuclear receptors; temporal regulation; morphogenesis;**
20 **collective migration; lumen formation**

21

22 **Summary**

23 During development, cells often undergo multiple, distinct morphogenetic
24 processes to form a tissue or organ, but how their temporal order and time interval are
25 determined remain poorly understood. Here we show that the nuclear receptors *E75*
26 and *DHR3* regulate the temporal order and time interval between the collective
27 migration and lumen formation of a coherent group of about 8 cells called border cells
28 during *Drosophila* oogenesis. In wild type egg chambers, border cells need to first
29 collectively migrate to the anterior border of oocyte before undergoing lumen
30 formation to form micropyle, the structure that is essential for sperm entry into the
31 oocyte. We show that *E75* is required for border cell migration and it antagonizes the
32 activity of *DHR3*, which is necessary and sufficient for the subsequent lumen
33 formation during micropyle formation. Furthermore, *E75*'s loss of function or *DHR3*
34 overexpression each leads to precocious lumen formation before collective migration,
35 an incorrect temporal order for the two morphogenetic processes. Interestingly, both
36 *E75* and *DHR3*'s levels are simultaneously elevated in response to signaling from the
37 *EcR*, a steroid hormone receptor that initiates border cell migration. Subsequently, the
38 decrease of *E75* levels in response to decreased *EcR* signaling leads to the
39 de-repression of *DHR3*'s activity and hence switch-on of lumen formation,
40 contributing to the regulation of time interval between collective migration and
41 micropyle formation.

42

43 **Introduction**

44 During development, a group or population of cells often has to undergo multiple,
45 distinct morphogenetic processes in a certain temporal order (e.g. A, then B...) to
46 form a tissue or organ (Webb and Oates, 2016). If the correct temporal order is not
47 followed (e.g. process B occurring before process A), that tissue or organ would not
48 form correctly (Rougvie, 2001; Thummel, 2001). Besides the correct order, the time
49 interval between two processes is another important aspect of the temporal control for
50 the morphogenetic processes. Making the interval too long or too short would also be
51 detrimental to the formation of the organ or tissue. Despite their importance in

52 development, our current understandings on how the temporal order and time
53 intervals are regulated and determined still remain very limited.

54

55 The somatic follicle cells of the *Drosophila* egg chamber have served as an excellent
56 model system to study multiple morphogenetic processes (Horne-Badovinac and
57 Bilder, 2005). Specifically, during stage 9 of oogenesis, a group of about 8 cells
58 detaches from the anterior follicle epithelium and undergoes collective migration
59 between the germ-line nurse cells in a posterior direction (Montell, 2003). By early
60 stage 10a, this coherent cluster of cells would have migrated a distance of about 150
61 μm in 6 hours, reaching the border between oocyte and nurse cells, hence the name
62 border cells. About four hours later, by stage 10b, the cluster of 8 border cells would
63 have migrated dorsally a short distance along the border, eventually stopping at the
64 dorsal-most position of the border. Three hours later, by stage 12 or 13, this border
65 cell cluster undergoes a second morphogenetic process to eventually form the tip of
66 micropyle, a tubular structure required for sperm entry into the mature oocyte
67 (Montell et al., 1992). Therefore, the formation of micropyle tip by border cells
68 requires two distinct morphogenetic processes in a certain temporal order, first the
69 well-studied, stereotyped, collective migration process and then a largely
70 uncharacterized morphogenetic process that transforms these border cells into the tip
71 of the tubular structure. Furthermore, an interval of about 16 hours exists between the
72 beginning of collective migration and the start of the micropyle formation
73 (Horne-Badovinac and Bilder, 2005). However, whether and how the temporal order
74 and the time interval between the two morphogenetic processes are regulated remain
75 largely unknown.

76

77 Previous studies have shed light on the temporal regulation of border cell migration.
78 The steroid hormone ecdysone, its receptor heterodimer Ecdysone Receptor (EcR)
79 and Ultraspiracle (USP), and their co-activator Taiman (Tai) had all been shown to be
80 required for the initiation of border cell migration (Bai et al., 2000; Jang et al., 2009).
81 Ecdysone and the EcR signaling had long been known to play important roles in

82 coordination of growth and developmental timing during embryogenesis, larval
83 molting and metamorphosis in *Drosophila* (Jia et al., 2017; Kozlova and Thummel,
84 2003; Yamanaka et al., 2013). Active form of ecdysone is also made in the adult
85 *Drosophila* ovaries to regulate progression of oogenesis (Buszczak et al., 1999;
86 Carney and Bender, 2000). 20-hydroxyecdysone, the active form of ecdysone, is
87 locally synthesized by the follicle epithelium in individual egg chambers and reaches
88 its highest levels around stages 9 and 10 (Domanitskaya et al., 2014; Margaret B et al.,
89 1989). Even small patches of wild type follicle cells in mosaic stage 9 egg chambers
90 were shown to produce a sufficient level of active ecdysone that allows the border
91 cells to begin migration (Domanitskaya et al., 2014). The sufficiency of ecdysone and
92 EcR signaling on initiation of border cell migration was further demonstrated by Jang
93 and coworkers, in which early expression of the activated form of the co-activator Tai
94 can precociously initiate border cell migration (Jang et al., 2009). However, what
95 cellular processes in the border cells are directly regulated by EcR signaling and
96 whether EcR also temporally regulates micropyle formation are currently unknown.

97

98 In this study, we show that E75 and DHR3, two nuclear receptors/transcription factors
99 downstream of EcR signaling, regulate both the temporal order and time interval
100 between border cell migration and micropyle formation. During border cell migration,
101 EcR signaling activates the expression of both E75 and DHR3, with E75 repressing
102 DHR3's function. Furthermore, de-repression of DHR3 function after completion of
103 border cell migration switches on lumen formation, turning the cluster of border cells
104 into the tip of micropyle. Such antagonistic relationship between E75 and DHR3
105 (while both under the control of EcR signaling) provides the regulatory mechanism of
106 temporal order and time interval between two distinct morphogenetic processes
107 essential for the formation of a functional micropyle.

108

109 **Results**

110

111 **RNAi Screen identifies E75 acting downstream of EcR signaling**

112 Ecdysone signaling was known to be critical for the temporal control of initiation of
113 border cell migration (Bai et al., 2000; Jang et al., 2009), but the cellular processes
114 directly regulated by EcR signaling are largely unknown. To identify these, we carried
115 out a small-scale RNAi screen of candidate genes that were previously reported to be
116 responsive to ecdysone in *Drosophila* larvae and pupae and in cell lines (Beckstead et
117 al., 2005; Gauhar et al., 2009; Sap et al., 2015). We first screened through the
118 well-established response genes of ecdysone signaling (Ashburner, 1976; Huet et al.,
119 1995; Yamanaka et al., 2013), including *E74*, *E75*, *E93*, *Br-c* and *DHR3*. Two to three
120 different RNAi lines for each gene were used to confirm that phenotypes were not due
121 to off-target effects, and two RNAi lines for the *EcR* gene were used as positive
122 controls. A border-cells specific Gal4 driver, *Slbo-Gal4*, was used to drive expression
123 of various *RNAi* transgenes in border cells beginning at late stage 8 of oogenesis,
124 before border cells initiate their migration at early stage 9. As expected, both *EcR*
125 *RNAi* lines (9327 and v35078 lines) resulted in phenotypes of strong migration delay
126 or block, consistent with the previous reported roles of EcR in initiating and
127 promoting border cell migration (Figures 1A, 1B and S1A-S1C) (Hackney et al., 2007;
128 Jang et al., 2009). In comparison, border cell clusters within the wild type control
129 stage 10 egg chambers almost always reached the 100% migration position, with only
130 6% of clusters displaying moderate delay (stopping at 75% migration position)
131 (Figures 1B and S1A-S1C). Interestingly, of all the five ecdysone response genes
132 tested, only *E75* displayed strong migration defects (Figures 1B and S1C). In fact, all
133 three RNAi lines (v44851, 26717, Thu1738) consistently resulted in severe migration
134 block and delay phenotypes, as compared to the control (Figures S1A and S1C). We
135 then screened an additional collection of 20 genes that were considered ecdysone
136 response genes or putative target genes of EcR/USP in recent reports (Beckstead et al.,
137 2005; Gauhar et al., 2009; Li and White, 2003). However, none of the genes, when
138 knocked down, displayed strong migration defects (Figure S1C). Only mild to
139 moderate migration phenotypes were observed in a few of the RNAi experiments.

140

141 We then proceeded to determine whether *E75* acts downstream of EcR to initiate and

142 promote border cell migration. Three distinct isoforms of *E75* (A, B, C) were shown
143 to be involved in different developmental and cellular processes and manifested stage-
144 and tissue-specific responses (Li et al., 2016; Terashima and Bownes, 2006), and the
145 sequences used in the three RNAi lines for *E75* are all within the common region and
146 would have knocked down all three isoforms. Therefore, we overexpressed each
147 isoform to test its individual rescue ability on border cell migration defects that were
148 caused by *EcR RNAi*. We found that *E75B* overexpression markedly rescued *EcR*
149 *RNAi*'s migration defects, whereas *E75C* displayed a much weaker rescue effect and
150 *E75A* showing no significant rescue (Figure 1B). Moreover, we found that *E75*'s
151 overall transcription levels (as represented by a previously used reporter *E75-lacZ*
152 (Manning et al., 2017) within border cells at stages 9 and 10 were much higher than
153 those at stage 8 (Figure 1C), consistent with ecdysone signaling being significantly
154 increased beginning at stage 9. And mosaic border cell clusters containing a clone of
155 *EcR RNAi* expressing cells demonstrate that *E75B* protein levels are drastically
156 decreased when *EcR* function is reduced (Figure 1D), indicating that *EcR* activity is
157 required for *E75B* expression during stage 9. Taken together, these results
158 demonstrate that *E75B* is the major downstream player, among the previously known
159 ecdysone response genes, to mediate *EcR*'s temporal control on border cell migration.
160 Consistently, a recent study using microarray analysis also identified *E75* as a target
161 gene that is responsive to ecdysone signaling in the migratory border cells (Manning
162 et al., 2017).

163

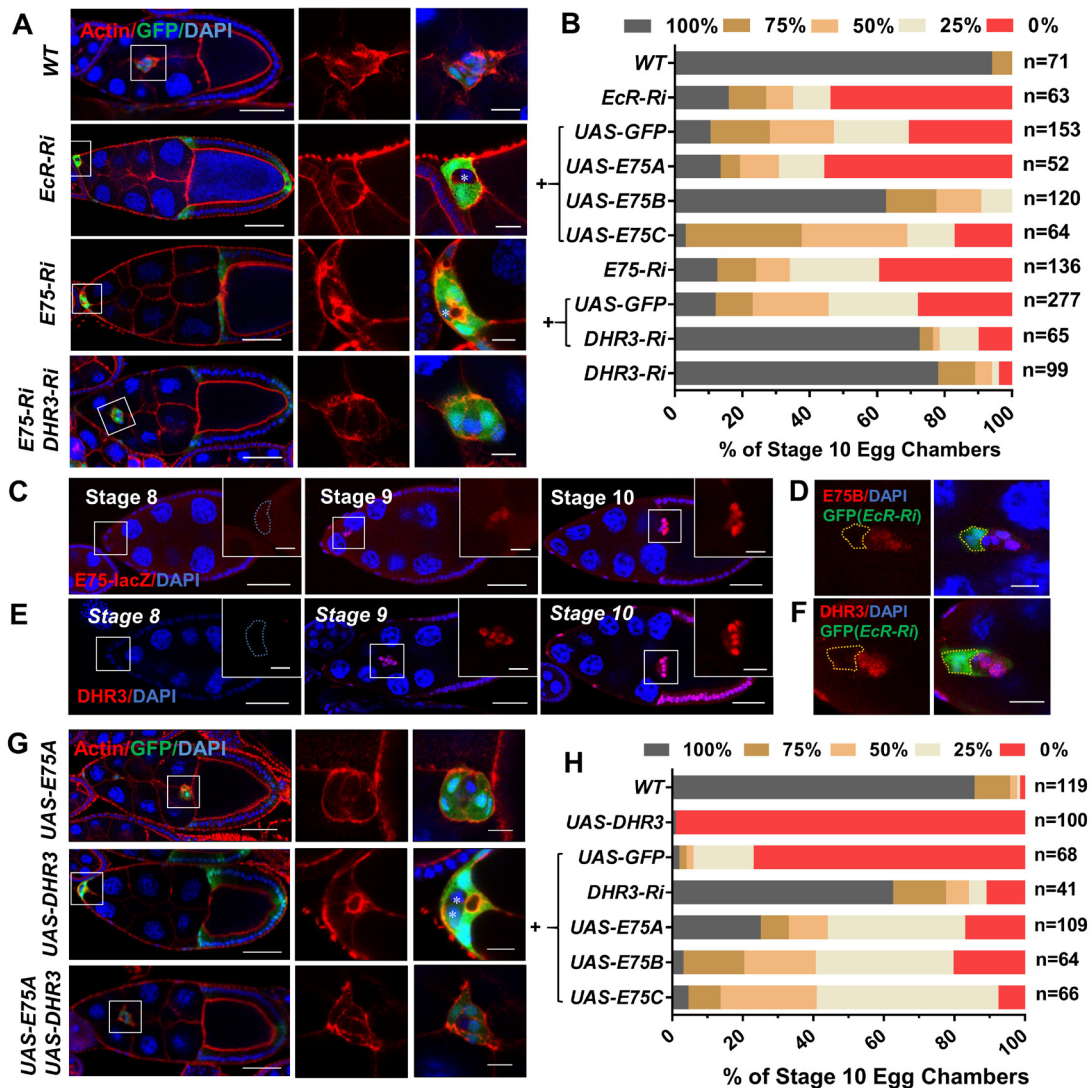


Figure 1. E75 antagonizes DHR3 during border cell migration

164

165

166

167

168

169

170

171

172

173

174

175

176

177

178

179

180

181

(A) Confocal images of egg chambers stained with phalloidin (red, for F-actin) and DAPI (blue, for nuclei) with indicated genotypes. The boxed regions are enlarged and shown to the right. Border cells expressing *EcR RNAi* displayed strong migration defects but exhibited similar morphology and F-actin distribution pattern to those of wild type (WT) border cells, whereas *E75 RNAi* border cells with migration defects displayed different morphology and F-actin distribution pattern from those of the *EcR RNAi* and WT border cells. Co-expression of *DHR3 RNAi* rescued *E75 RNAi*'s morphology and F-actin defects. *Ri* is the abbreviation for *RNAi* for this and all subsequent figures. Posterior is to the right and anterior is to the left for this and all subsequent figures. (B) Quantification of border cell migration with indicated genotypes. *EcR-Ri* denotes *EcR RNAi*, and "+" indicates that these genotypes include both *EcR RNAi* and one of the denoted genotypes (*UAS-GFP*, *UAS-E75A*, *UAS-E75B*, and *UAS-E75C*). The "+" below *E75 RNAi* indicates that these genotypes includes both *E75 RNAi* and one of the denoted genotypes (*UAS-GFP*, *DHR3 RNAi*). The stock used for *E75 RNAi* is v44851, which is used for all the other experiments unless noted otherwise. The x-axis denotes the percentage of stage 10 egg chambers examined for

182 each genotype that exhibited various degrees of migration, as represented by the five
183 color-coded bars (see Figures S1B and S1C for details). The 100% migration category
184 (grey) indicates completion of migration, whereas 0% (red) indicates severe migration
185 block. And the 25%, 50% and 75% categories indicate various degrees of migration
186 delay. (C, E) Confocal images displaying β -galactosidase staining (C) and DHR3
187 staining (E) of stages 8, 9 and 10 egg chambers. Boxed region is enlarged to the right,
188 showing a high-magnification view of the border cells. (D, F) Confocal images
189 showing antibody staining of E75B (D) and DHR3 (F) of individual stage 10 border
190 cell clusters with flip-out clones expressing *EcR RNAi* (*EcR-Ri*). The flip-out clones
191 (labeled by GFP and encircled by yellow dotted lines) clearly displayed marked
192 reduction of E75B and DHR3 respectively. (G) Border cells overexpressing *DHR3*
193 exhibited severe defects in migration and morphology, which could be rescued by
194 co-expression of *E75A*. Border cells with *E75A* overexpression alone displayed wild
195 type phenotype. * (in A and G) indicates polar cells that are labeled by absence of
196 GFP. (H) Quantification of rescue of border cell migration defects as resulted from
197 *DHR3* overexpression. “+” indicates that these genotypes include both *UAS-DHR3*
198 and one of the denoted genotypes (*UAS-GFP*, *DHR3 RNAi*, *UAS-E75A*, *UAS-E75B*,
199 and *UAS-E75C*). Scale bars: 50 μ m in (A, C, E, G), 10 μ m for high-magnification
200 views in (A, C-F, G). See also Figures S1 and S2.

201

202 **E75 antagonizes DHR3’s function during collective migration of border cells**

203 During metamorphosis, ecdysone-activated EcR turns on the expression of E75B,
204 which then binds to DHR3 and antagonizes its activity (White et al., 1997). E75B and
205 DHR3 are both nuclear receptors/transcription factors and are both induced by
206 ecdysone, and E75B’s inhibition of DHR3 function leads to suppression of DHR3’s
207 transcriptional activation of its target genes essential for metamorphosis (Caceres et
208 al., 2011; Reinking et al., 2005; White et al., 1997). To determine whether
209 antagonistic interaction also exists between E75 and DHR3 during border cell
210 migration, we co-expressed *DHR3 RNAi* and *E75 RNAi* in border cells. We found that
211 DHR3 reduction strongly rescued *E75 RNAi*’s migration defects (Figures 1A and 1B),
212 as well as the morphological defects of border cells (Figure 1A, also described in the
213 section below). On the other hand, overexpression of *DHR3* resulted in similar
214 phenotypes of migration and morphology to those of *E75 RNAi* (Figures 1G and 1H),
215 with *DHR3* overexpression’s defects more severe than those of *E75 RNAi* (Figures 1B,
216 1H, S3A and S3B). Furthermore, *E75* overexpression can in turn suppress *DHR3*
217 overexpression’s severe defects (Figures 1G and 1H), with all three of its isoforms

218 (E75A, E75B, E75C) displaying similar suppressing abilities. This is consistent with
219 previous reports that both E75A and E75B isoforms can heterodimerize with DHR3 to
220 inhibit DHR3's transcription activation ability (Sullivan and Thummel, 2003; White et
221 al., 1997). Lastly, we showed that DHR3's levels were also increased in border cells
222 beginning at stage 9 (Figure 1E), similar to E75's temporal expression pattern (Figure
223 1C), and its levels also depended on EcR's activity (Figure 1F). Together, these data
224 demonstrate an antagonistic relationship between E75 and DHR3 during border cell
225 migration, with both their expressions activated by EcR during the migratory process.

226

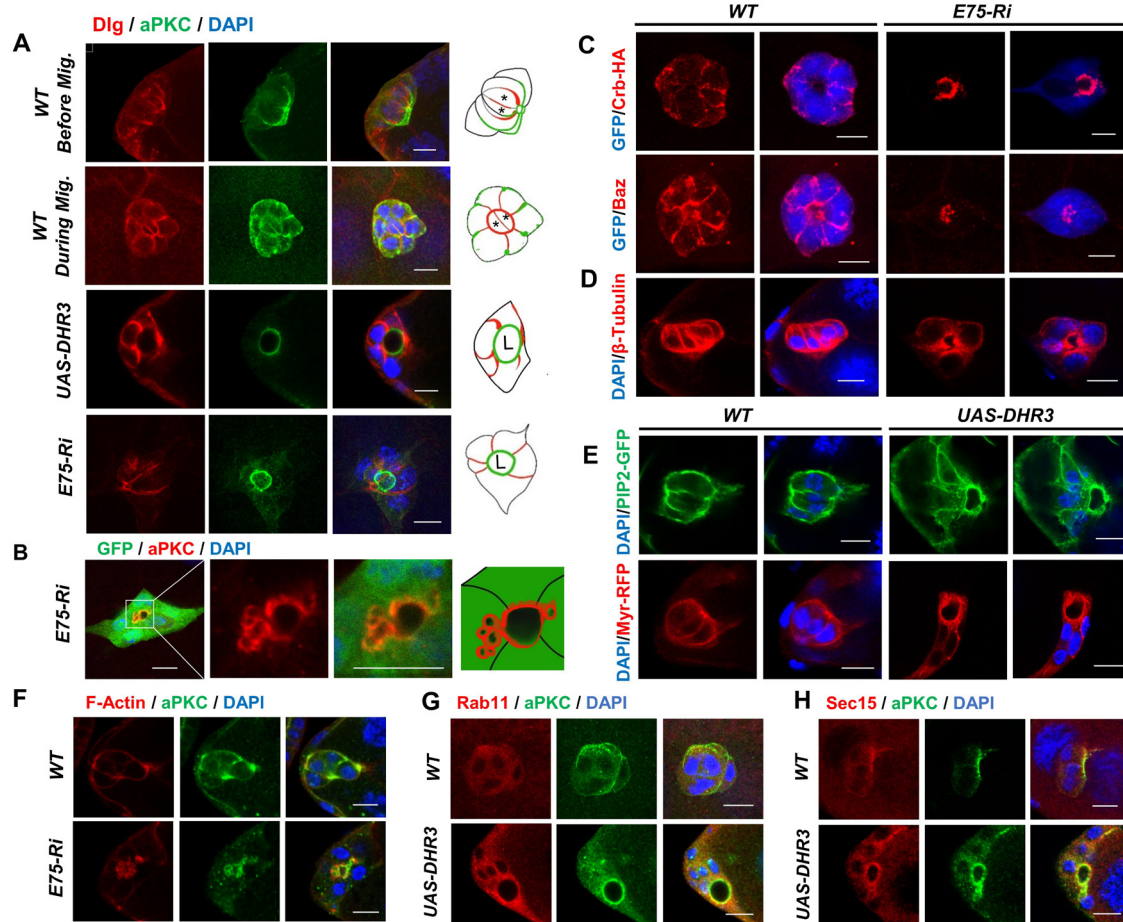
227 Conversely, we found that expressing *E75 RNAi* (stock 26717) or *DHR3* in border
228 cells significantly reduced the level of ecdysone response activity or EcR signaling
229 (Figures S2A-S2C and S2F), which is represented by expression levels of *EcRE-lacZ*,
230 a common reporter of EcR activity used in previous studies (Jang et al., 2009; Koelle
231 et al., 1991). Moreover, expression of *DHR3 RNAi* could rescue *E75 RNAi*'s
232 *EcRE-lacZ* expression levels (Figures S2D-S2F). These data indicate that E75 can
233 exert a positive feedback on EcR signaling by antagonizing DHR3's inhibition effect
234 on EcR signaling. This conclusion is consistent with previous studies that showed
235 DHR3 physically interacted with EcR and suppressed its activity (Lam et al., 1997;
236 White et al., 1997). These results suggest that one of the means that E75 mediates
237 EcR's migration-promoting function is through E75's positive feedback on EcR
238 signaling.

239

240 **E75 antagonizes DHR3's function in lumen formation during border cell** 241 **migration**

242 We noted that border cell clusters with *E75* knockdown or *DHR3* overexpression
243 displayed different morphology and F-actin staining pattern from border cells with
244 reduced EcR function (Figures 1A and 1G), as indicated by our *EcR RNAi* result and
245 previous reports (Hackney et al., 2007; Jang et al., 2009). The delayed border cell
246 clusters with *EcR RNAi* often displayed a coherent and front-polarized morphology
247 with F-actin enriched in the front periphery of the cluster, similar to that of the wild

248 type clusters (Figure 1A). On the contrary, *E75 RNAi* or *DHR3* overexpressing border
249 cells lost the front-polarized cluster morphology that is characteristic of front-back
250 polarity, and F-actin is instead enriched in the center of the cluster in a ring-like
251 structure (Figures 1A and 1G), which is unique and never observed in any of the
252 previously reported mutant phenotypes of border cells (to our knowledge). Closer
253 examination revealed that this unique structure is not within individual border cell's
254 cytoplasm but is instead composed of portions of outer border cells' inside
255 membranes, which are joined together to form a continuous supra-cellular ring
256 (Figures 2A-2E). Moreover, this supra-cellular structure is also enriched with
257 molecules that are typically associated with apical membranes (aPKC, Crb, Baz/Par3,
258 PIP2-GFP reporter) (Figures 2A, 2C and 2E) but not with lateral membranes (Dlg)
259 (Figures 2A). A typical supra-cellular ring encloses a space that resembles a lumen
260 with significant depth (about 5-10 μm , Movie S1) in the center of cluster, effectively
261 displacing the two central polar cells to the side and underneath (Figures 2A, 1A and
262 1G; marked by *). The strong and specific enrichment of apical markers such as
263 aPKC in the membranes enclosing the luminal space suggests that the border cell
264 cluster has undergone a lumen formation process to become a tubular structure with
265 the apical membrane facing the central lumen. Interestingly, the *E75 RNAi* border
266 cells displayed a range of lumen-like phenotypes. Half of them (50.0%) showed a
267 clear lumen phenotype that is similar to that of the *DHR3* overexpressing border cells,
268 while majority of the rest (39.0%) exhibited little luminal space and discontinuous
269 apical membrane patches as labeled by aPKC (Figure S3A and S3B), which resemble
270 the previously reported structure of pre-apical patches (PAP) that are present during
271 the intermediate stages of *de novo* lumen formation in several model systems (Bryant
272 et al., 2010; Ferrari et al., 2008; Yang et al., 2013). These moderate phenotypes may
273 reflect incomplete lumen formation or the intermediate stages of lumen formation in
274 the border cells, while the large lumen structure from almost all of the *DHR3*
275 overexpressing border cells and half of the *E75 RNAi* border cells may indicate
276 complete lumen formation.



277

278 **Figure 2. E75 loss of function and DHR3 overexpression lead to precocious**
 279 **lumen formation of the border cells**

280 (A) The first two rows show confocal images of wild type border cells before
 281 migration (first row, early stage 9) and during migration (second row, mid stage 9)
 282 respectively. Before migration, the apical (stained with aPKC) and lateral (stained
 283 with Dlg) membranes of border cell cluster points to the posterior direction (to the
 284 right), with apical membrane more posterior than lateral membrane. During migration,
 285 the orientation of border cell cluster undergoes a 90 degree turn, resulting in the
 286 apical-lateral axis being perpendicular to the posterior direction (to the right). The two
 287 central polar cells are outlined by strong staining of Dlg and marked with * in the
 288 diagrams to the right. The last two rows depict border cells with *E75 RNAi* or *DHR3*
 289 overexpression that failed to migrate and instead formed lumen (marked with “L” in
 290 the diagrams) that is enclosed by aPKC stained membrane. Dlg staining is restricted
 291 to membranes between adjacent border cells. The first and last rows are resulted from
 292 maximum projection of z-stacks of confocal sections, the others are single confocal
 293 sections. (B-E) Images of border cells labeled with aPKC (B), Crb-HA and Baz (C),
 294 β-tubulin (D) staining, and PIP2-GFP and Myr-RFP (E) fluorescence, as resulted from
 295 *E75 RNAi* or *DHR3* overexpression. DAPI labels all nuclei. PIP2-GFP serves as a
 296 reporter for PIP2-enriched membrane (PLCδ-PH-GFP, see Methods for details), and
 297 Myr-RFP (myristoylated RFP) serves as a general membrane marker. (F-H) Images
 298 showing co-staining of aPKC with phalloidin (F-actin, F), Rab11 (recycling

299 endosome marker, G), and Sec15 (exocyst component, H), as resulted from *E75 RNAi*
300 or *DHR3* overexpression. Scale bars, 10 μ m for all panels. See also Figure S3.

301

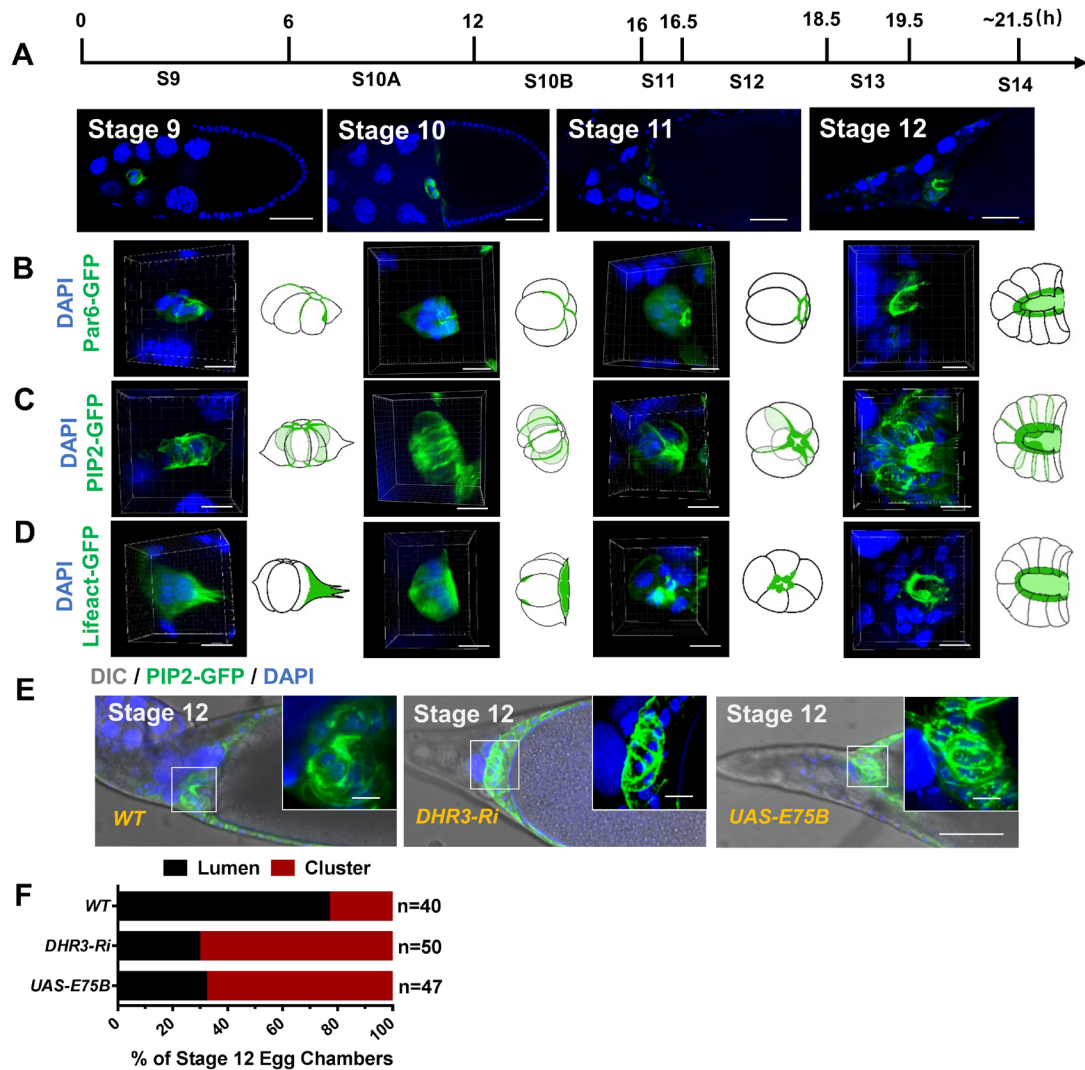
302 Formation of a tube and its enclosing lumen from non-epithelial cells is referred to as
303 *de novo* lumen formation (Sigurbjornsdottir et al., 2014), which is a fundamental
304 morphogenetic process central to animal development. Extensive studies in various *in*
305 *vitro* and *in vivo* model systems have revealed that the initial stage of *de novo* lumen
306 formation involves establishment of a new apical-basal polarity, which requires
307 re-routing of multiple cellular processes and components including polarized
308 intracellular trafficking, polarized actin and microtubule cytoskeleton, polarized
309 distribution of apical markers, and newly synthesized membrane (Akhtar and Streuli,
310 2013; Datta et al., 2011; Sigurbjornsdottir et al., 2014). We found that in addition to
311 the re-distribution of apical markers to the lumen-facing membrane, the intracellular
312 traffic as well as cytoskeleton was also dramatically re-organized in the *E75 RNAi* or
313 *DHR3* overexpressing border cells. Staining with Rab11 and Sec15 antibodies
314 revealed that recycling endosome and exocyst were enriched in the cytoplasmic
315 regions near the lumen-facing apical membrane, indicating a polarized transport
316 toward the lumen (Figures 2G and 2H). Furthermore, F-actin and, sometimes, aPKC
317 were observed localizing to large vacuole-like compartments adjacent to the
318 lumen-facing membrane (Figures 2B and 2F), suggesting that these large vesicles
319 could be in the process of fusing with the adjacent apical membrane. This
320 phenomenon was similar to previous reports of VACs (vacuolar apical compartments)
321 forming in the MDCK cells that are undergoing *de novo* lumen formation (Brignoni et
322 al., 1993; Vega-Salas et al., 1988). In addition, the actin and microtubule
323 cytoskeletons were re-organized in such a way that they are now mostly localized in
324 and adjacent to the lumen-facing membrane. Interestingly, β -tubulin was re-organized
325 into a distribution pattern that seems to radiate away from the central lumen (Figure
326 2D). Lastly, marked increase of intracellular membrane levels as indicated by
327 Myr-RFP and PIP2-GFP was observed in the cytoplasm of *DHR3* expressing border
328 cells, suggesting that high levels of newly synthesized membranes are needed for

329 formation and expansion of lumen-facing membrane (Figure 2E). Taken together,
330 these results indicate that during border cell migration *E75* acts to suppress *DHR3*'s
331 lumen formation function, which includes re-routing of endocytic recycling,
332 re-distribution of apical markers, re-polarization of actin and microtubule
333 cytoskeletons, and increased levels of membrane components.

334

335 **DHR3 is later required for the formation of micropyle tip**

336 We next sought to understand why *E75* needs to suppress *DHR3*'s lumen formation
337 function during border cell migration. After border cells finished their anterior
338 migration to the border at stage 10A, they will further migrate a short distance
339 dorsally and finally stop at the dorsal border between nurse cells and oocyte at stage
340 10B. About three hours later, around stages 12 and 13, this cluster of border cells will
341 undergo a morphogenetic transformation to form part of the micropyle, which is a
342 tubular structure essential for sperm entry (Montell et al., 1992). Such a
343 morphogenetic process is not well characterized and understood. Therefore, we
344 wonder whether the lumen-forming phenotype from *E75* knockdown or *DHR3*
345 over-activation represents the precocious occurrence of the morphogenetic event
346 involved in micropyle formation. If that is the case, *E75* may be actually preventing a
347 late morphogenetic process from occurring earlier (i.e. before or during border cell
348 migration). Therefore, *E75* and *DHR3* may function together to keep the correct
349 temporal order between the two morphogenetic processes. To address this possibility,
350 we first sought to characterize and understand the process that enables wild type
351 border cell cluster to be transformed into the tip of micropyle.



352

353 **Figure 3. DHR3 is required for border cells' lumen formation in the micropyle at**
 354 **stage 12**

355 (A-D) A time course of developing wild type egg chambers at stages 9, 10, 11 and 12.
 356 3-D reconstruction of z-stacks of confocal section (see Methods for details) reveals
 357 the change of morphology from a cluster to the anterior portion of the tubular
 358 micropyle (B-D). See also Movies S2-S4 that are generated from the 3-D
 359 reconstruction. Par6-GFP (B), Lifact-GFP (C) and PIP2-GFP (D) fluorescence
 360 displays a dynamic remodeling of apical polarity, F-actin and PIP2-enriched
 361 membrane in border cells during micropyle formation. The genotype of the PIP2-GFP
 362 reporter (Cliffe et al., 2017) is detailed in Methods. (E, F) *DHR3 RNAi* and *E75B*
 363 overexpression each caused disruption of lumen formation, as compared to the
 364 morphology of wild type border cells (outlined by PIP2-GFP) at stage 12. Their
 365 cluster or lumen morphology are quantified in (F). 76.6% of stage 12 wild type border
 366 cell clusters displayed obvious lumen morphology, whereas 70.4% of *DHR3 RNAi*
 367 and 68.0%, of *E75B* overexpression displayed cluster morphology, which is
 368 characteristic of the wild type border cells at stage 10 (C). Scale bars, 50 μ m in (A, E),
 369 10 μ m in high-magnification views in (B-E). See also Figures S3 and S4.

370

371 Collective migration of border cells has been extensively studied, but the
372 morphogenetic process that turns the border cells into micropyle tip is little studied.
373 Previous work by Montell and coworkers first demonstrated that border cells develop
374 into the tip of micropyle and contribute to the cellular process thought to maintain a
375 functional opening, while the centripetal follicle cells form the bulk of the micropyle
376 structure. Furthermore, in the absence of border cells, a slightly smaller micropyle
377 structure could still form, but it lacks the functional opening required for sperm entry
378 (Montell et al., 1992). We sought to describe and characterize such morphogenetic
379 process in details, using markers of actin cytoskeleton, membrane and apical polarity
380 (Figures 3A-3D, Movies S2-S4). Similar to migratory border cells at stage 9, border
381 cells at stage 10 (a period of about 10 hours, Figure 3A) mostly retain the coherent
382 cluster morphology as well as the distribution pattern of F-actin and apical polarity
383 proteins. During stages 9 and 10, Par6-GFP was shown to localize between adjacent
384 border cells in a thin section of junctional region (Figure 3B, Movie S2), which was
385 subsequently retracted and significantly shortened during stage 11 (a period of about
386 0.5 hour). During stage 12, Par6-GFP localization is further remodeled, with its
387 pattern shifted from junctional region between adjacent border cells to the membrane
388 facing the lumen-like cavity (Figure 3B, Movie S2). Consistently, Lifeact-GFP and a
389 PIP2 membrane reporter (PIP2-GFP, Cliffe et al., 2017) both demonstrate a similar
390 remodeling in their distribution patterns from stage 9 to stage 12, with Lifeact-GFP
391 and PIP2-GFP highly enriched in the same membrane region enclosing the luminal
392 space in wild type border cells at stage 12 (Figures 3C and 3D, Movies S3 and S4). A
393 very small percentage of wild type stage 11 or 12 egg chambers would contain border
394 cells that failed to migrate properly and reach the oocyte border (Figures S4A-S4E).
395 Interestingly, we found that those stages 11 and 12 border cells with migration defects
396 also displayed lumen formation that was accompanied by the remodeling of apical
397 markers, F-actin, and PIP2-enriched membrane and was similar to the DHR3-induced
398 lumen formation process at stages 9 and 10 (Figures S4A-S4E). This result indicates
399 that the remodeling process is autonomously initiated in border cells and is under

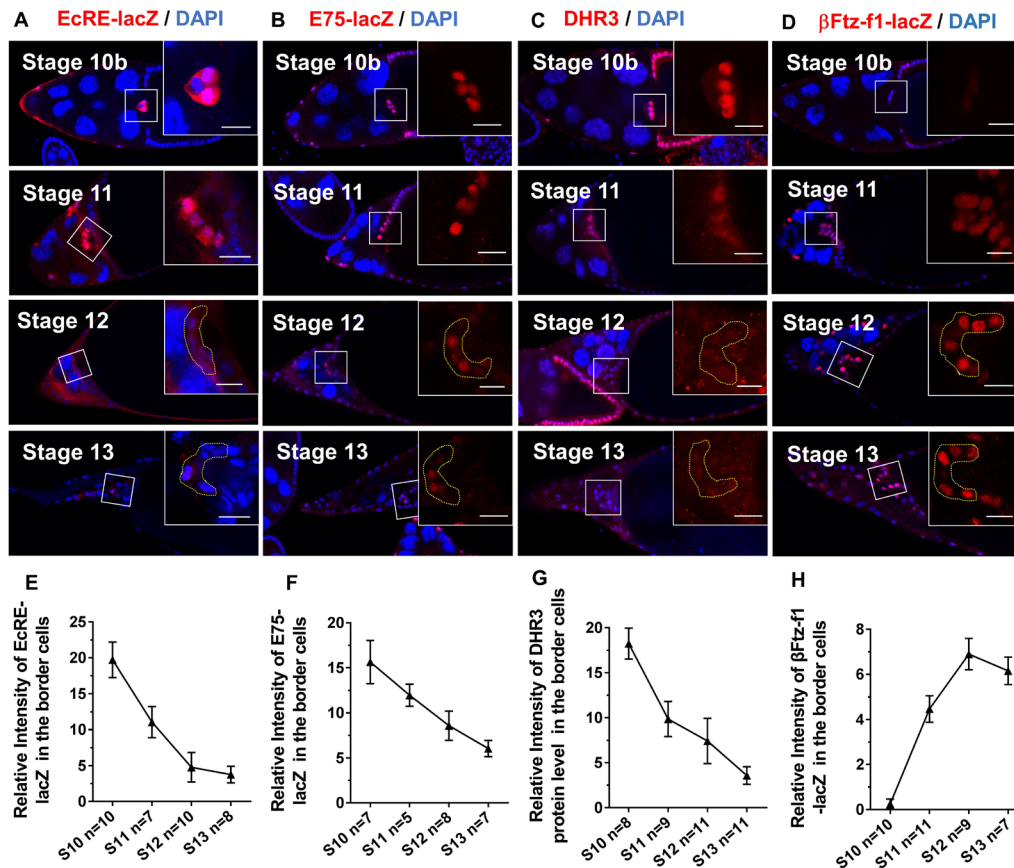
400 strict temporal control. Finally, *DHR3* knockdown or *E75* overexpression each led to
401 disruption of the remodeling process (Figures 3E and 3F). As shown by the PIP2-GFP
402 marker (Figure 3E), most of *DHR3 RNAi* or *E75* overexpressing border cell clusters at
403 stages 12 and 13 displayed a cluster morphology that is characteristic of border cells
404 at stages 9 and 10 (Figure 3C, Movie S3), where the PIP2-GFP is broadly localized in
405 membranes between adjacent border cells. Consequently, these border cells failed to
406 develop into the anterior tip of micropyle that surrounds a lumen-like cavity.
407 Together, these results demonstrate that DHR3 activity is required for the
408 morphogenetic process of lumen formation that is essential to micropyle formation.
409 Interestingly, the morphogenetic remodeling process involved in micropyle formation
410 is similar to the DHR3-induced lumen formation process occurred precociously in
411 border cell cluster during stages 9 and 10, suggesting that DHR3 is not only required
412 but also sufficient for all the remodeling events necessary for lumen formation.
413 Indeed, random ectopic expression of *DHR3* in small clones of follicle cells by the
414 Flip-out technique could sometimes induce formation of lumen-like structures
415 enclosed by *DHR3* expressing follicle cells (Figure S3C), supporting the above idea.

416

417 **Reduction of EcR signaling and E75 levels causes de-repression of DHR3 activity**

418 We next sought to understand how DHR3 function is temporally regulated to limit its
419 lumen forming activity only to the period of micropyle formation and not to the
420 period of collective migration. We reasoned that DHR3's activity in border cells has
421 to be inhibited by *E75* during stages 9 and 10, as shown by our results above (Figure
422 1). Afterward, DHR3's activity would need to be de-repressed beginning at stage 11 to
423 start the morphogenetic process of lumen formation. We already showed that DHR3
424 function is antagonized by *E75*, and that both *E75* and *DHR3* are expressed by EcR
425 during border cell migration at stage 9. We then examined the temporal expression
426 patterns of *E75* and *DHR3* as well as the levels of EcR signaling. We found that EcR
427 signaling, as reflected by its well-established reporter *EcRE-lacZ*, reached its highest
428 levels during stage 10B, and then dramatically declined from stage 11 to stage 13
429 (Figures 1C, 4A and 4E). Accordingly, both expression levels of the *E75-lacZ* reporter,

430 which reflects the transcription levels of *E75* (Figures 4B and 4F), and the protein
 431 levels of DHR3 as detected by DHR3 antibody also decreased from stage 11 to stage
 432 13 (Figures 4C and 4G). These results suggest that as ecdysone signaling decrease
 433 dramatically (beginning at stage 11) *E75* level should also decrease to a low level (at
 434 stages 11 and 12), which may be below the threshold level for inhibition of DHR3's
 435 activity. To test this possibility, we need a good activity reporter for DHR3's function.



436

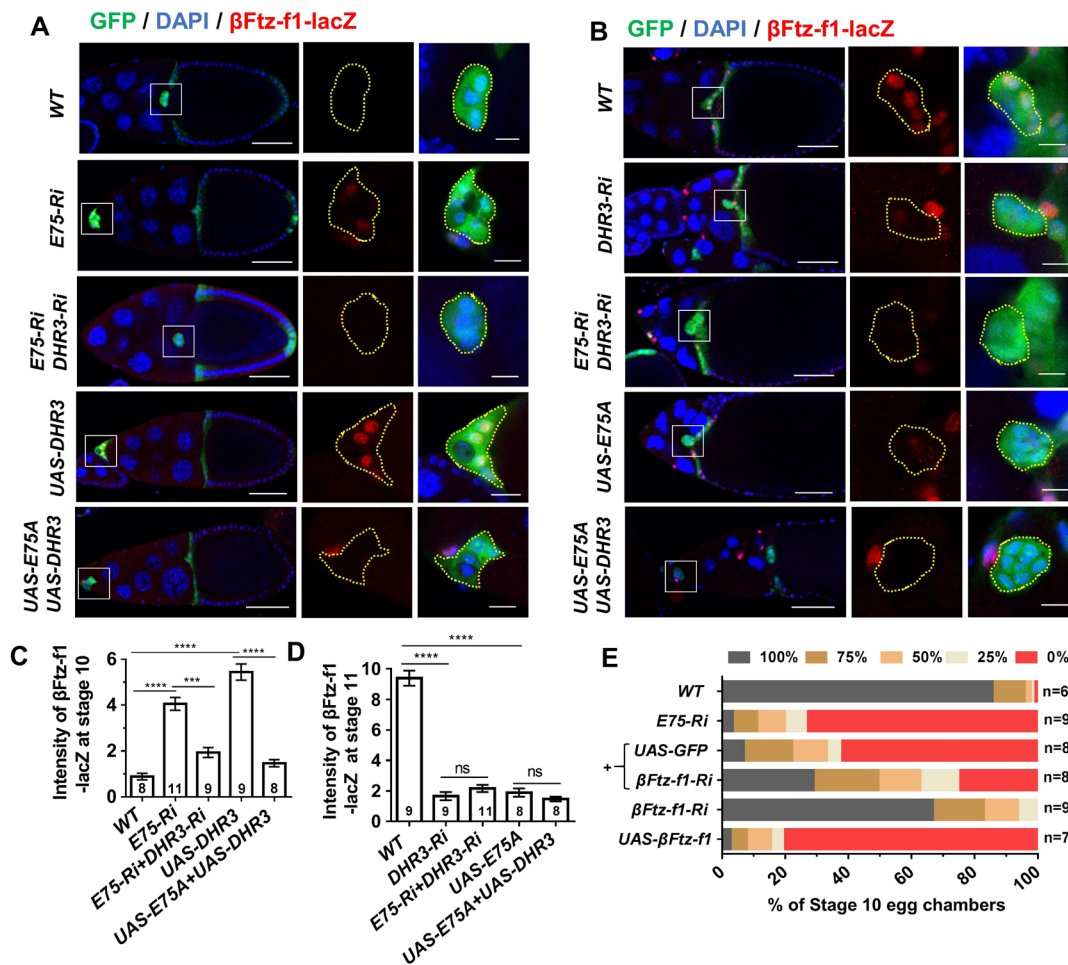
437 **Figure 4. Temporal expression patterns of EcRE-lacZ, E75-lacZ, DHR3 and**
 438 **β -Ftz-f1-lacZ from stage 10b to stage 13**

439 (A-D) Confocal images showing antibody staining of β -gal that is expressed by the
 440 *EcRE-lacZ* reporter (A), *E75-lacZ* enhancer trap (B), and *β -Ftz-f1-lacZ* enhancer trap
 441 (D), as well as antibody staining of DHR3 (C), from stage 10b to stage 13. Boxed
 442 regions are enlarged and shown at the right of all panels. Areas encircled by yellow
 443 dotted lines (based on labeling of GFP as expressed by *slbo-Gal4*) highlight the
 444 border cell clusters (A-D) at stages 12 and 13. Scale bars, 10 μ m. (E-F) Quantification
 445 of antibody staining of border cell clusters in (A-D) from stage 10b to stage 13. The
 446 number of egg chambers examined (n) for each stage is given at the x-axis. Statistical
 447 analysis was performed using two-tailed Student's *t*-test. Error bars indicate S.E.M.
 448 See also Figure S5.

449

450 Previous literatures indicate that DHR3's immediate downstream target gene during
451 metamorphosis is *βFtz-fl* (Geanette T. Lam1, 1997; Jia et al., 2017; Kageyama et al.,
452 1997), whose expression levels serve as a readout for DHR3 activity. We obtained an
453 enhancer trap line for *βFtz-fl*, *βFtz-fl-lacZ*, which has a *lacZ* containing P-element
454 inserted in the 5' UTR region of the gene and supposedly could reflect the
455 transcription level of *βFtz-fl*. We found that its expression could serve as a bona fide
456 reporter for DHR3 activity, based on the following results. First, *βFtz-fl-lacZ*
457 expression is initially at non-detectable levels at stages 9 and 10A (Figure S5A), and
458 at very low levels at stage 10B (Figures 4D and 4H), then it abruptly reaches much
459 higher levels at stages 11, 12 and 13 (Figure 4D, H). Therefore, *βFtz-fl-lacZ*'s
460 temporal expression pattern is highly consistent with our above prediction about the
461 temporal regulation of DHR3 activity. Second, *DHR3* overexpression led to
462 precocious expression of *βFtz-fl-lacZ* within border cells during stages 9 and 10,
463 whereas co-expression of *E75B* and *DHR3* suppressed such precocious expression
464 (Figures 5A and 5C). Conversely, *DHR3 RNAi*, *E75B* overexpression, or *E75B* and
465 *DHR3* co-expression, each inhibited *βFtz-fl-lacZ*'s normal expression in border cells
466 during stage 11 (Figures 5B and 5D). Furthermore, *DHR3* overexpression in the
467 follicle cells at the stage 9, when *βFtz-fl-lacZ* is not normally expressed, ectopically
468 induced *βFtz-fl-lacZ*'s expression in the follicle cells (Figure S5B). Third, expression
469 of *βFtz-fl-RNAi* in the background of *E75 RNAi* partially rescues border cell's
470 migration defects (Figure 5E and Figure S6A), suggesting that *βFtz-fl* functions
471 downstream of DHR3. Lastly, expressing *βFtz-fl-RNAi* in the border cells resulted in
472 the disruption in the formation of micropyle tip, similar to the loss-of-function defects
473 of *DHR3 RNAi* (Figures S6B and S6C). On the other hand, overexpression of *βFtz-fl*
474 in stage 10 border cells resulted in actin-enriched patches that are similar to PAPs
475 from moderate *E75 RNAi* defects (Figures S3A and S3B), suggesting an incomplete
476 lumen forming phenotype. Taken together, these results support the conclusion that
477 reduction in EcR signaling and E75 levels leads to de-repression of DHR3 activity (as
478 represented by the *βFtz-fl-lacZ* reporter) beginning at stage 11, which serves to
479 switch on lumen formation for micropyle formation (during stages 11 to 13).

480 Moreover, β Ftz-f1 acts downstream of DHR3 to mediate micropyle formation.



481

482 **Figure 5. β -Ftz-f1 acts downstream of DHR3 and its expression serves as a**
 483 **reporter of DHR3 activity**

484 (A) β -Ftz-f1-lacZ levels in border cells at stage 10 as represented by β -gal antibody
 485 staining. Compared to wild type (WT) control, *E75 RNAi* and *DHR3* overexpression
 486 both resulted in significant increase of β -Ftz-f1-lacZ levels (quantified in C), while
 487 double knock down of *E75* and *DHR3* (*E75 Ri* + *DHR3 Ri*) and overexpression of
 488 both *DHR3* and *E75* (*UAS-DHR3* + *UAS-E75*) abolished the increase (quantified in
 489 C). (B) β -Ftz-f1-lacZ levels in border cells at stage 11 as represented by β -gal staining.
 490 Compared to wild type (WT) control, *DHR3 RNAi* and *E75* overexpression both
 491 resulted in significant reduction of β -Ftz-f1-lacZ levels (quantified in D). Yellowed
 492 dotted lines (A, B) outline individual border cell clusters, as labeled with GFP
 493 expressed by *Slbo-Gal4*. Boxed regions (A, B) are enlarged and shown at the right of
 494 all panels. Scale bars, 50 μ m for egg chambers, 10 μ m for border cells. (C, D)
 495 Quantification of β -Ftz-f1-lacZ levels. The number of egg chambers examined for
 496 each genotype is indicated within its corresponding column. Statistical analysis was
 497 performed using two-tailed Student's *t*-test. Error bars indicate S.E.M. **, $P < 0.01$;
 498 ***, $P < 0.001$; ****, $P < 0.0001$; ns, not significant. (E) Quantification of rescue of
 499 border cell migration defects of *E75 RNAi* by co-expression of *β -Ftz-f1 RNAi*.
 500 Represented images for the indicated genotypes are shown in Figure S6A. See also

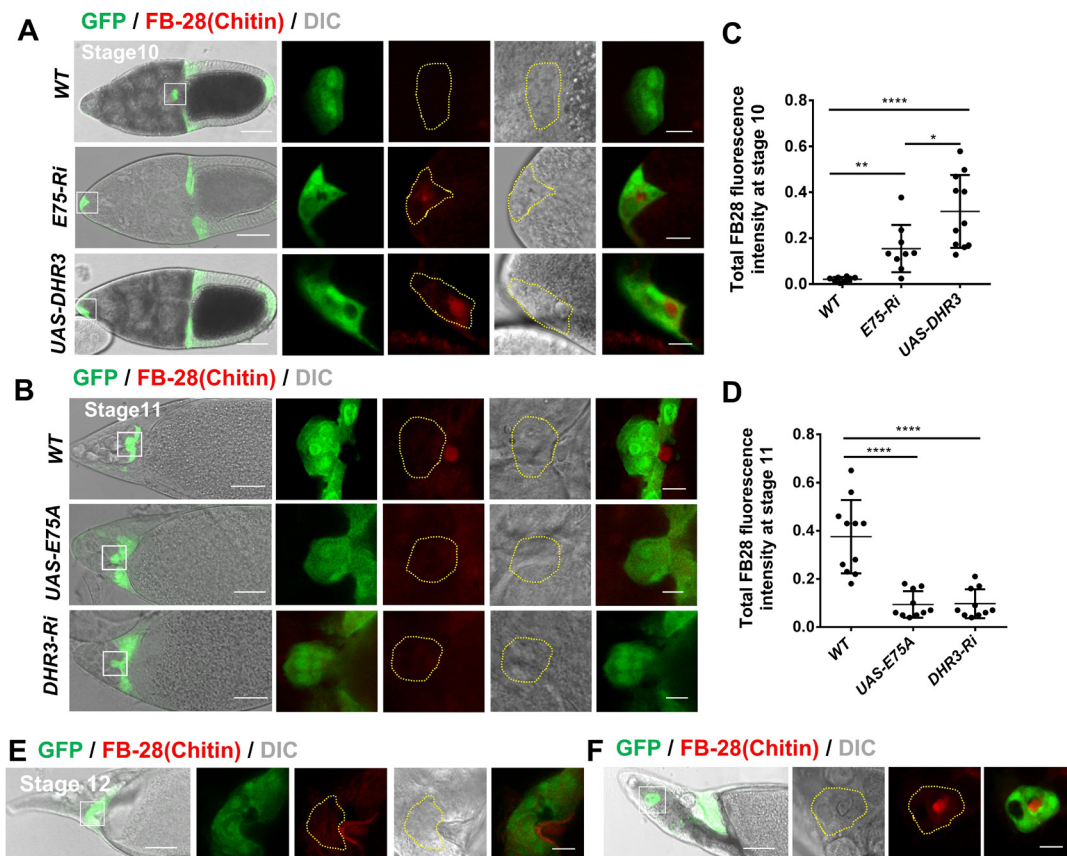
501 Figure S6.

502

503 **DHR3 is required and sufficient for chitin secretion into the lumen**

504 An essential feature of *de novo* lumen formation in the vertebrates is the secretion of
505 glycoprotein such as the negatively charged podocalyxin into the lumen to keep the
506 lumen membranes apart and promote the expansion of luminal space (Bryant et al.,
507 2014; Strilic et al., 2010). Although *Drosophila* does not possess a podocalyxin
508 homolog, the tube formation during *Drosophila* tracheal development requires the
509 secretion of chitin into the lumen (Devine et al., 2005). Chitin is a long-chain polymer
510 of N-acetylglucosamine, which is also a primary component of the *Drosophila*
511 exoskeleton (Moussian et al., 2005; Zhu et al., 2016). We then proceeded to determine
512 whether chitin is present in the lumen enclosed by the border cells and whether DHR3
513 acts to promote secretion of chitin into the lumen. Interestingly, we found that chitin
514 (labeled by FB-28) is only present in the extracellular space adjacent to wild type
515 border cells during and after stage 11 (Figures 6B, 6D, 6E and S7E), whereas it is not
516 present around the border cells before stage 11 (Figures 6A, 6C and S7E). A very
517 small percentage of wild type stage 12 egg chambers would contain border cells that
518 failed to migrate properly and reach the oocyte border, and we found that chitin is
519 present within the lumen surrounded by those border cells (Figure 6F). Together,
520 these results indicate that chitin is present in the lumen within the border cell cluster.
521 In addition, the temporal and localization patterns of chitin suggest that it is secreted
522 by border cells beginning at stage 11 during lumen formation for the micropyle tip.
523 Furthermore, we found that expressing *E75 RNAi* or *DHR3* specifically in the border
524 cells (by *slbo-Gal4*) each resulted in chitin being precociously localized within the
525 lumen of border cell clusters that failed to migrate to the oocyte border at stage 10
526 (Figures 6A and 6C), indicating that DHR3 activation is sufficient to induce chitin
527 secretion. On the contrary, *DHR3* knockdown or *E75* overexpression led to loss of
528 extracellular chitin near border cells at stage 11 (Figures 6B and 6D), indicating
529 DHR3 is required for chitin secretion by the border cells. Together, these results
530 indicate that DHR3 activity is necessary and sufficient for chitin secretion by the

531 border cells during lumen formation. To further test whether β Ftz-f1 is also sufficient
 532 for chitin secretion, we examined and found no chitin secretion in β Ftz-f1
 533 overexpressing border cells at stage 10 (Figures S7A and S7C). This result could be
 534 due to the aforementioned fact that β Ftz-f1 overexpression only resulted in PAP
 535 (incomplete lumen formation, Figure S6A). Hence, it is conceivable that chitin
 536 secretion can only occur after lumen formation progresses to a certain degree. On the
 537 other hand, we found that β Ftz-f1 is required for chitin secretion by the border cells
 538 during micropyle formation (Figures S7B and S7D), similar to DHR3's role (Figures
 539 6B and 6D). These results suggest that β Ftz-f1 may act downstream of DHR3 to
 540 partially mediate DHR3's chitin secretion role.



541

542 **Figure 6. DHR3 is necessary and sufficient for chitin secretion by the border cells**
 543 **during lumen formation**

544 (A, B) Confocal and DIC images showing chitin staining in stage 10 (A) and stage 11
 545 (B) egg chambers. Chitin is labeled with the Fluorescent Brightener 28 (FB28) dye.
 546 (A) Chitin was not detected within or adjacent to wild type (WT) border cells at stage
 547 10, whereas *E75* RNAi and *DHR3* overexpression in the border cells resulted in
 548 precocious secretion of chitin to the lumen (quantified in C). (B) Starting at stage 11,

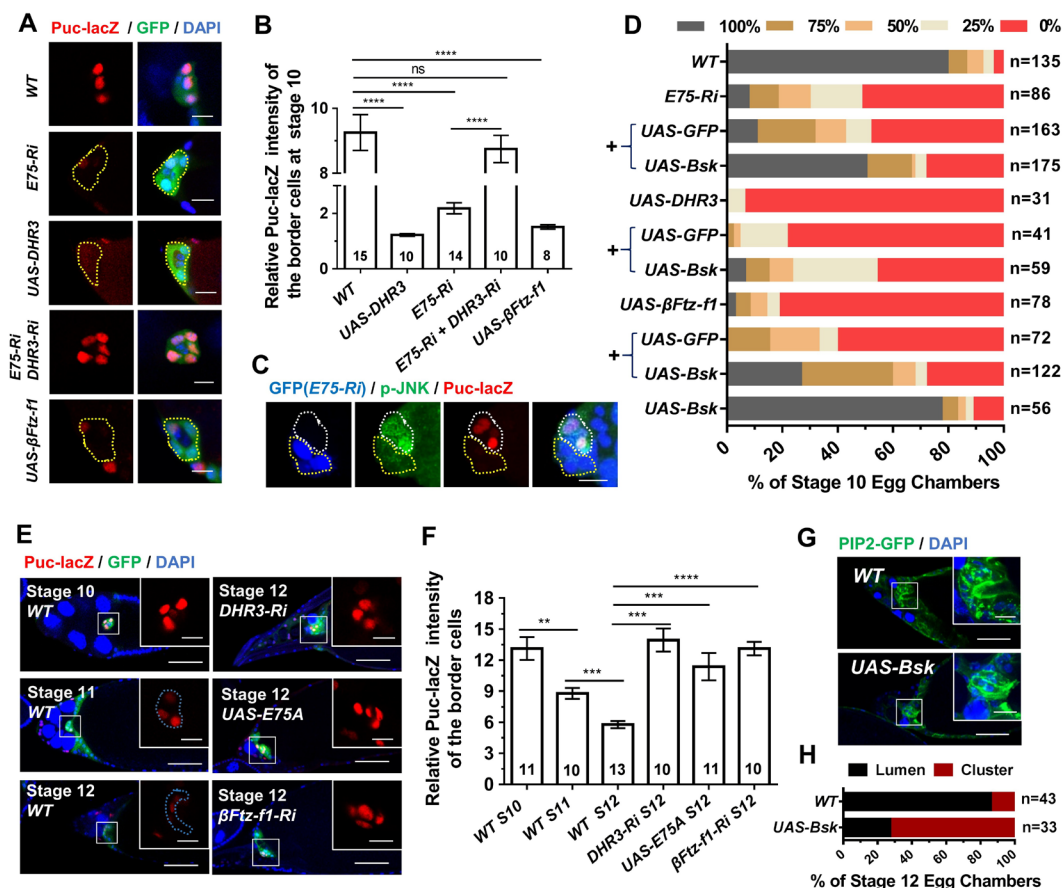
549 chitin was detectable adjacent to WT border cell cluster, but *DHR3* RNAi or *E75*
550 overexpression abolished chitin staining (quantified in D). Yellow dotted lines outline
551 individual border cell clusters as labeled with GFP expressed by *Slbo-Gal4*. Scale bars,
552 50 μm for egg chambers, 10 μm for border cells. (C, D) Quantification of chitin levels
553 of border cells for the indicated genotypes. (E) At stage 12, chitin was detectable in
554 the lumen of micropyle, where wild type border cells had completed their migration.
555 (F) In stage 12 wild type border cells that exhibited migration defects, chitin was
556 detected in the lumen enclosed by border cells. Statistical analysis was performed
557 using two-tailed Student's *t*-test. Error bars indicate S.E.M. **, $P < 0.01$; ****,
558 $P < 0.0001$. See also Figure S7.

559

560 **DHR3 and β Ftz-f1 suppress JNK signaling in the border cells**

561 Lastly, we sought to explore what signaling pathways DHR3 regulates in border cells.
562 We tested reporters for a number of signaling pathways previously known to play
563 essential roles in the border cells, including JAK/STAT (Beccari et al., 2002; Silver et
564 al., 2005), Notch (Wang et al., 2007), JNK (c-Jun N-terminal kinase) (Llense, 2008;
565 Melani et al., 2008) and Dpp (Luo et al., 2015). Among them, JNK was the only
566 signaling found to be severely affected by *E75* knockdown or DHR3 overexpression
567 (Figure S8A). JNK signaling pathway was previously reported to be required for
568 cell-cell adhesion between adjacent border cells during their collective migration
569 (Llense, 2008; Melani et al., 2008). Staining for *Puc-lacZ*, a widely used reporter for
570 JNK signaling, revealed that both *E75 RNAi* and *DHR3* overexpression caused strong
571 reduction of *Puc-lacZ* reporter activity in stage 10 (Figures 7A-7C), indicating that
572 increased DHR3 activity suppresses JNK signaling. Indeed, knockdown of *DHR3* in
573 the background of *E75 RNAi* rescued the level of *Puc-lacZ* expression back to the
574 wild type level in stage 10 (Figures 7A and 7B). Furthermore, overexpressing *bsk*
575 (encoding *Drosophila* JNK) in the background of *E75 RNAi* or *DHR3* overexpression
576 partially rescued the severe migration defects and precocious lumen formation of
577 border cells that were resulted from *E75* loss of function (Figure 7D and S8B).
578 Together, these results demonstrate that reduction of *E75* or increase of DHR3 activity
579 leads to downregulation of JNK signaling in the migratory border cells at stages 9 and
580 10. We next tested whether JNK signaling was negatively regulated by DHR3 and
581 β Ftz-f1 during micropyle formation. We showed that in the wild type the level of JNK

582 signaling was reduced from stage 10 to stage 11, and then further reduced from stage
 583 11 to stage 12 (Figures 7E and 7F). In stage 12 border cells, *DHR3* knockdown, *E75*
 584 overexpression, and β *Ftz-f1* knockdown each increased the originally low JNK
 585 signaling to a much higher level, which is similar to the level at stage 10 (Figures 7E
 586 and 7F). These results suggest that JNK signaling needs to be suppressed in order for
 587 lumen formation to occur properly during stages 11 and 12. Indeed, overexpression of
 588 *bsk* and hence increase of JNK signaling resulted in disruption of lumen formation
 589 during formation of the micropyle tip at stage 12 (Figures 7G and 7H). Taken together,
 590 these results suggest that JNK-mediated cell adhesion between border cells is
 591 temporally and differentially regulated during two different morphogenetic processes:
 592 collective migration and micropyle formation, and that its downregulation by *DHR3*
 593 and β *Ftz-f1* is essential for lumen formation in the latter process.



594

595 **Figure 7. *DHR3* and β *FTZ-f1* downregulate JNK signaling in the border cells.**
 596 (A, B) *Puc-lacZ* expression levels in migratory border cells at stage 9 or 10 as
 597 represented by β -gal antibody staining. *E75 RNAi*, *DHR3* and β *FTZ-f1* overexpression

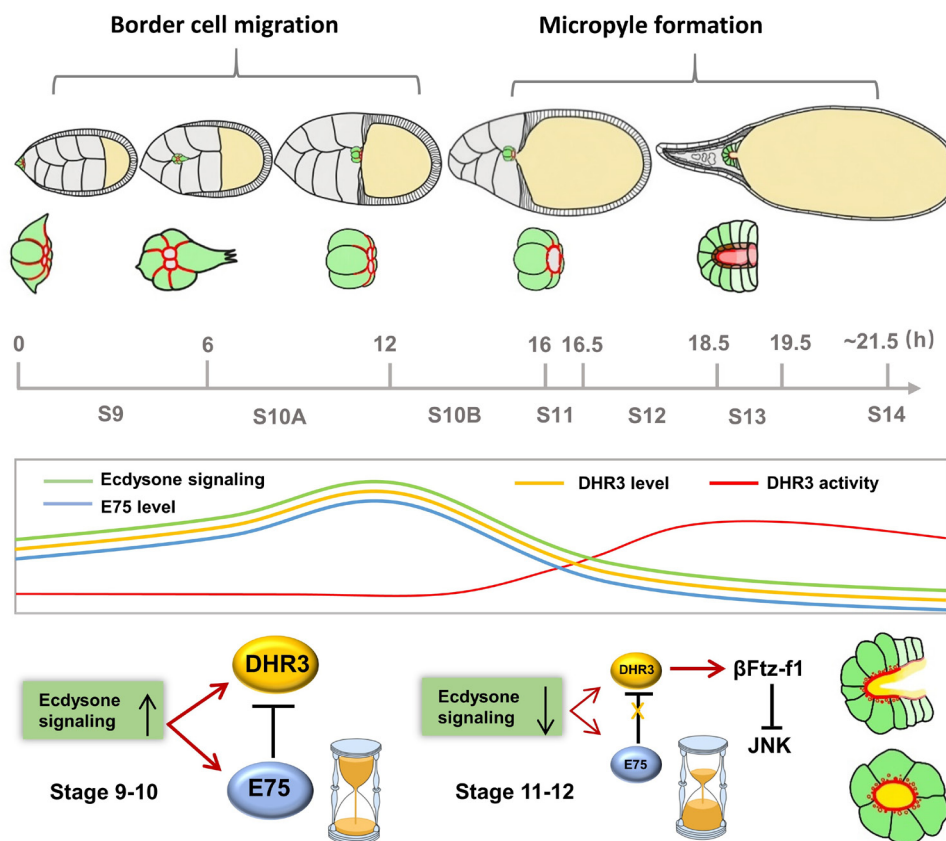
598 each resulted in strong and significant decrease of *Puc-lacZ* levels as compared to
599 wild type (WT) control (quantified in B), while coexpression of *DHR3 RNAi* and *E75*
600 *RNAi* returns the *Puc-lacZ* levels to that of WT (quantified in B). (C) A mosaic border
601 cell cluster containing a clone of *E75 RNAi* expressing cells (marked by GFP, outlined
602 with yellow dotted line), which exhibited reduction of *Puc-lacZ* and p-JNK levels as
603 compared to those in the adjacent wild type cells (no GFP, outlined with white dotted
604 line). (D) Quantification of partial rescue of border cell migration defects of *E75*
605 *RNAi*, *DHR3* overexpression, and *βFTZ-fl* overexpression by coexpression of *bsk*. (E,
606 F) *Puc-lacZ* expression levels in WT border cells decreased from stage 10 to stage 12,
607 while expression of *DHR3 RNAi*, *E75A* and *βFTZ-fl RNAi* elevated *Puc-lacZ* levels
608 in border cells at stage 12. The results are quantified in (F). (G, H) *bsk* overexpression
609 caused disruption of lumen formation, as compared to morphology of wild type
610 border cells (outlined by PIP2-GFP) at stage 12. Their cluster or lumen morphology
611 are quantified in (H). 86.0% of stage 12 wild type border cells displayed obvious
612 lumen morphology, whereas 72.7% of *bsk* overexpressing cells displayed cluster
613 morphology, which is characteristic of the wild type border cells at stage 10.
614 Statistical analysis was performed using unpaired two-tailed Student's *t*-test. Error
615 bars indicate S.E.M. **, P<0.01; ***, P<0.001; ****, P<0.0001; ns, not significant.
616 Scale bars, 10 μm. See also Figure S8.

617

618 Discussion

619 We demonstrate that two nuclear receptors, *E75* and *DHR3*, are critical for temporal
620 coordination of two very different morphogenetic processes of the border cell cluster,
621 namely its collective migration and its lumen formation. First, our results revealed
622 that the levels of *E75* and *DHR3* (in response to ecdysone) are the underlying control
623 of the temporal order (Figure 8). Strong loss of function of *E75* or *DHR3*
624 overexpression disrupts the temporal order and causes lumen formation to occur first.
625 Consequently, collective migration could not take place afterward, because of the
626 unique nature of the lumen structure, which precludes migration from occurring.
627 Second, levels of *E75* and *DHR3* together with the antagonism between the two
628 nuclear receptors underlie the mechanistic control of time interval between the two
629 morphogenetic processes (Figure 8). *E75* acts as a molecular timer. Its expression
630 level determines the length of interval between migration and lumen formation
631 (Figure 8). Very little *E75* (strong loss-of-function) causes lumen formation to occur
632 before migration could take place, effectively resulting in no interval between the two
633 morphogenetic processes. Moderate *E75* loss-of-function phenotype demonstrates that

634 collective migration could take place at early stage 9 (Figures S3A and S3B), but
 635 accompanied with a precocious occurrence of lumen formation at late stage 9 or stage
 636 10, indicating a shortened interval. On the other hand, too much *E75* (*E75*
 637 overexpression) results in reduced occurrence of lumen formation at stage 12 or 13
 638 (Figure 3F), suggesting an expanded interval. Finally, it is important to note that
 639 delayed wild type border cells that supposedly contain the wild type levels of *E75* and
 640 *DHR3* exhibit a normal time interval (Figures S4 and 7F). During tissue or organ
 641 formation, it is not uncommon for a certain cell population to undergo two vastly
 642 different morphogenetic processes. This study provides a novel mechanistic insight
 643 into the molecular machinery that coordinates both the order and time interval
 644 between morphological processes.



645

646 **Figure 8. Model of how *E75* and *DHR3* temporally coordinate the migration and**
 647 **lumen formation of border cells.** See description in the Discussion section for
 648 details.

649

650 Our study also uncovers a surprising mechanism of how a nuclear receptor controls
651 the process of de novo lumen formation. DHR3 seems to act as a potent switch or
652 inducer for lumen formation since it is necessary and sufficient for lumen formation
653 of border cells both during stage 9 and during stages 11-13. Activation of DHR3
654 function in border cells seems to simultaneously induce multiple cellular processes
655 that were previously demonstrated to be essential for *de novo* lumen formation in
656 other systems (Sigurbjornsdottir et al., 2014), including re-routing of endocytic
657 recycling, re-distribution of apical markers, re-polarization of actin and microtubule
658 cytoskeletons, and increased synthesis of membrane components. In addition, DHR3
659 is necessary and sufficient for the secretion of chitin into the lumen of border cells
660 both at stage 9 and at stage 12. Chitin had been previously shown to be required for
661 tube expansion and maturation during *Drosophila* tracheal morphogenesis (Devine et
662 al., 2005). Its function seems to provide an extracellular matrix support (Moussian et
663 al., 2006; Wang et al., 2006). The mechanism by which chitin affects tube
664 morphogenesis remains poorly understood. How DHR3 induces chitin synthesis and
665 secretion and whether chitin is required for lumen formation and tube maturation in
666 micropyle remain to be further determined. Furthermore, we demonstrate that DHR3's
667 lumen-inducing function is mainly mediated through β Ftz-f1, a nuclear receptor and
668 transcription factor that has been well established to be DHR3's immediate target
669 gene during metamorphosis. However, β Ftz-f1 does not seem to mediate all of
670 DHR3's functions since *β Ftz-f1* overexpression could not induce complete lumen
671 structure and chitin secretion, suggesting that other factors downstream of DHR3 may
672 also contribute to lumen formation. Lastly, we show that JNK signaling is
673 downregulated by DHR3 and β Ftz-f1, suggesting that cell adhesion between adjacent
674 border cells needs to be reduced during lumen formation. This is consistent with the
675 idea that remodeling of apical polarity, cytoskeleton and membrane during lumen
676 formation may require down-regulation of cell-cell adhesion. Given the multiple
677 functions as demonstrated for DHR3, it will be interesting to test whether these lumen
678 inducing functions will be conserved in other developmental contexts in *Drosophila*
679 and vertebrate. Interestingly, previous studies reported that the mammalian homolog

680 of DHR3, ROR α , was enriched in human mammary duct, and its inactivation
681 impaired polarized acinar morphogenesis (Xiong et al., 2012; Xiong and Xu, 2014),
682 suggesting a similar role in vertebrate.

683

684 Although treated as an excellent model system for collective migration, border cells'
685 physiological function during oogenesis is to make a functional opening within the
686 micropyle for sperm entry. How the border cell cluster develops into the anterior tip
687 of the tubular structure of micropyle is poorly understood. Our study reveals a
688 dynamic remodeling of apical polarity molecules, F-actin, and PIP2-enriched
689 membrane, which is consistent with the process of *de novo* lumen formation. The
690 functional roles of DHR3, β Ftz-f1, EcR, E75 and JNK during micropyle formation, as
691 demonstrated by our study, provide the first detailed analysis of this morphogenetic
692 process. We suggest that in addition to collective migration, border cells could also
693 serve as a model system to study *de novo* lumen formation in *Drosophila*.

694

695 **Author Contributions**

696 Conceptualization, J.C., X.W., S.L. and G.E; Methodology, X.W., J.C., and H.W.;
697 Investigation, X.W., H.W., L.L; Resources, S.L. and G.E.; Visualization, X.W. and
698 H.W.; Writing, J.C., X.W. and G.E., Supervision, J.C. and H.W.

699

700 **Competing interests**

701 The authors declare no competing financial interests.

702

703 **Funding**

704 This work is supported by grants from the National Natural Science Foundation of
705 China (31970743, 31571435) and Natural Science Foundation of Jiangsu Province
706 (BK20171337) to J.C., grants from the National Natural Science Foundation of China
707 (31900563) and Natural Science Foundation of Jiangsu Province (BK20190303) to
708 H.W. G.E. is supported by grants from the Canadian Institute for Health Research

709 (CIHR; MOP-148560), the Natural Sciences and Engineering Research Council of
710 Canada.

711

712 **Acknowledgments**

713 We thank Henry Krause and Oren Schuldiner for E75 related flies and antibodies,
714 Carl Thummel for DHR3 antibody. We also thank Jacques Montagne, Juan Huang,
715 Lei Xue, Xiaobo Wang, Zizhang Zhou, the Bloomington Drosophila Stock Center,
716 Tsinghua University Fly Stock Center, National Institute of Genetics Stock Center
717 (Japan), and Vienna Drosophila RNAi Center for other fly stocks. We thank Zhenji
718 Gan for critical comments.

719

720

721 **Methods and Materials**

722 **Fly stocks**

723 Flies were cultured and maintained on standard cornmeal media with sugar and yeast
724 at 25°C. Progenies of crosses between *UAS-RNAi* or *UAS-transgenes* and *Slbo-Gal4*
725 were cultured at 29°C for two days for specific gene's knockdown and overexpression.
726 For moderate knockdown or overexpression, flies were cultured at 29°C for only one
727 day or cultured at 25°C, as indicated in the figure legends. To generate flip-out clones
728 of border cells and follicle cells, female flies were heated-shocked for 3 minutes at
729 37°C and then kept at 29°C for 1 day before dissection.

730 Fly stocks listed below were obtained from different labs and stock centers, including
731 Bloomington Stock Center (BDSC), National Institute of Genetics Stock Center,
732 Japan (NIG), Vienna Drosophila RNAi Center (VDRC) and Tsinghua Fly Center
733 (THFC).

734

735 **Fly stocks:**

STOCK #	SOURCE	IDENTIFER
---------	--------	-----------

UAS-E74 RNAi	VDRC	v45900
UAS-E74 RNAi	NIG	6273R-3
UAS-E74 RNAi	NIG	6285-1R-1
UAS-E75 RNAi	VDRC	v44851
UAS-E75 RNAi	BDSC	26717
UAS-E75 RNAi	THFC	THU1738
UAS-E93 RNAi	VDRC	v45855
UAS-E93 RNAi	VDRC	v45856
UAS-Br-C RNAi	BDSC	38526
UAS-Br-C RNAi	NIG	11514R-3
UAS-EcR RNAi	VDRC	v35078
UAS-EcR RNAi	BDSC	9327
UAS- DHR3 RNAi	VDRC	v12204
UAS- DHR3 RNAi	VDRC	v106837
UAS- crol RNAi	VDRC	v104313
UAS- Hr39 RNAi	VDRC	v37694
UAS- Hr39 RNAi	VDRC	v37695
UAS- Su RNAi	VDRC	v105675
UAS- Hr4 RNAi	VDRC	v101856
UAS- cact RNAi	BDSC	34775
UAS- E2F RNAi	VDRC	v15886
UAS- Sox14 RNAi	VDRC	v107146
UAS- Sox14 RNAi	VDRC	v10856
UAS- Sox14RNAi	BDSC	26221
UAS- brat RNAi	VDRC	v105054
UAS- Kr-h1RNAi	VDRC	v51282
UAS- Kr-h1RNAi	VDRC	v31333
UAS- Ef4A RNAi	VDRC	v45686
UAS- Ef4A RNAi	VDRC	v107846
UAS- Kis RNAi	VDRC	v109414
UAS- E63F-1RNAi	VDRC	v26899
UAS- Cyp4e2 RNAi	VDRC	v108025
UAS- bip1 RNAi	VDRC	v26104
UAS- Impl2 RNAi	VDRC	v106543
UAS- Past1 RNAi	VDRC	v22253
UAS- srp RNAi	VDRC	v109521
UAS- Eip78C RNAi	BDSC	28851
UAS- Eip78C RNAi	BDSC	26718
UAS- vrille RNAi	VDRC	v5650
UAS- β Ftz-f1 RNAi	BDSC	27659
UAS- β Ftz-f1 RNAi	VDRC	v104463
Slbo-gal4,UAS-GFP/Cyo	BDSC	6458
PIP2-GFP Reporter	Gift from HsinHo Sung and Pernille	N/A

(Slbo-PH(PLC δ)-4xGFP,Ubi-His-tone-RFP,Slbo-gal4,Upd-Gal4, UMAT-Lyn-tdTomato)	Roth (Cliffe et al., 2017), used in Figures 3, 7, S4 and S6 and Movie S3	
Ay-Gal4,UAS-GFP	BDSC	4411
Slbo-lacZ,Slbo-Gal4/Cyo	Gift from Pernille Roth	N/A
UAS-E75A	Gift from Henry M. Krause (Caceres et al., 2011)	N/A
UAS-E75B.Flag	Gift from Oren Schuldiner (Rabinovich et al., 2016)	N/A
UAS-E75C.Flag	Gift from Oren Schuldiner (Rabinovich et al., 2016)	N/A
UAS-DHR3	Gift from Henry M. Krause (Caceres et al., 2011)	N/A
UAS-Bsk.B	BDSC	9310
UAS- β Ftz-f1	BDSC	64290
UAS-Lifeact.GFP	BDSC	35544
UAS-PLC δ -PH-GFP	BDSC (used in Figure 2E)	39693
UAS-Par6.GFP	BDSC	65847
UAS-Myr.RFP	BDSC	7119
UAS-GFP	BDSC	4776
UAS-Puc	Gift from Lei Xue (Ma et al., 2011)	N/A
EcRE-lacZ	BDSC	4517
E75-lacZ	BDSC	11712
β Ftz-f1-lacZ	BDSC	11598
Puc ^{E69} -lacZ	Gift from Xue Lei (Ma et al., 2013)	N/A
E(sp)m7-lacZ	From Zizhang Zhou and Qing Zhang (Tseng, 2014)	N/A
Dad-lacZ	From Zizhang Zhou and Qing Zhang (Ninov, 2010)	N/A
10xStat-GFP	BDSC	26197
Crb-HA	Gift from Juan Huang (Huang et al., 2009)	N/A

736

737 **Antibodies**

ANTIBODY	SOURCE	IDENTIFER
mouse anti-lacZ(1:100)	DSHB	Cat#401-a
Mouse anti-Dlg (1:100)	DSHB	Cat#4F-3
Mouse anti β -tubulin (1:100)	DSHB	Cat#E7
Rabbit anti-P-JNK (1:100)	Promega	Cat#V7932

Mouse anti-HA probe (1:100)	Santa Cruz	Cat#F-7
Mouse anti-Rab11 (1:200)	Santa Cruz	Cat#Sc-6565
Rabbit anti-aPKC ζ (1:100)	Santa Cruz	Cat#C-20
Rat anti-E-cadherin (1:50)	DSHB	Cat#5D3
Rabbit anti-Bazooka (1:400)	Gift from A. Wodarz	N/A
Donkey anti-Sec15 (1:200)	Gift from Hugo J.Bellen	N/A
mouse anti-E75B(1:20)	gift from Henry M. Krause(Caceres et al., 2011)	N/A
Rabbit anti-DHR3 (1:100)	gift from Carl S. Thummel(Ruaud et al., 2010)	N/A
Cy5 AffiniPure Goat Anti-Rabbit IgG	Jackson ImmunoResearch	Cat#111-495-144
Cy3-AffiniPure Goat Anti-Rat IgG	Jackson ImmunoResearch	Cat#112-165-167
Cy3-AffiniPure Goat Anti-Mouse IgG	Jackson ImmunoResearch	Cat#115-165-166
Cy5-AffiniPure Donkey Anti-Guinea Pig IgG	Jackson ImmunoResearch	Cat#706-605-148

738

739 **Chemicals**

CHEMICAL	SOURCE	IDENTIFER
Regular insulin	Novo Nordisk	NDC# 0169-2313-21
Fluorescent Brightener 28	Sigma-Aldrich	Cat#F3543
DAPI	Santa Cruz Biotechnology	Cat#sc-3598;
TRITC-conjugated Phalloidin	Sigma-Aldrich	Cat#P1951

740

741 **Software**

SOFTWARE	SOURCE	IDENTIFER
GraphPad Prism 6	www.graphpad.com	N/A
Image J	http://imagej.nih.gov/ij	N/A
Leica confocal software	http://softadvice.informer.com/Leica_Confocal_Software.html	N/A

Imaris 7.2.3	http://www.bitplane.com	N/A
--------------	---	-----

742

743 **Method Details**

744 **Immunostaining**

745 Female flies were raised on fresh food with yeast at 29°C for 2 days. Ovaries were
746 dissected in PBS, and then fixed in 100ul devitellinizing buffer (7% formaldehyde)
747 and 600ul heptane, with strong shaking for 10 min, then washed 3 x10min with PBS,
748 and 3x10 min with PBST. For egg chamber staining, egg chambers were blocked with
749 10% goat serum in PBST for 30 min after fixed and washed, and then incubated with
750 primary antibody at 4°C overnight. Ovary samples were then washed 3x10 min with
751 PBST, blocked with 10% goat serum in PBST for 30min, incubated with secondary
752 antibody at 1:200 in PBST for 2 hours. DAPI was added and stained for 30 min
753 during secondary staining. Lastly, ovaries were washed again with 10 min PBST for
754 three times, mounted on microscope slide with 40% glycerol. Primary antibodies used
755 include mouse anti-lacZ (1:100,401-a, DSHB), mouse anti-E75B (1:20, gift from
756 Henry M. Krause)(Caceres et al., 2011), rabbit anti-DHR3 (1:100, gift from Carl S.
757 Thummel)(Ruaud et al., 2010), Rabbit anti-p-JNK (1:50, Promega, V7932), Rat
758 anti-E-cad (1:50, 5D3, DSHB), Rabbit anti-PKC ζ (C-20, 1:100, Santa Cruz), mouse
759 anti-Dlg (4F3, 1:100, DSHB) , mouse anti-HA(1:100, F-7, Santa Cruz), rabbit
760 anti-Baz (1:400, gift from A. Wodarz). Secondary antibodies were used including Cy5
761 AffiniPure Goat Anti-Rabbit IgG, Cy3-AffiniPure Goat Anti-Rat IgG, Cy3-AffiniPure
762 Goat Anti-Mouse IgG, Cy5-AffiniPure Donkey Anti-Guinea Pig IgG (1:200, Jackson
763 ImmunoResearch). Confocal images were obtained with Leica SP5 confocal
764 microscopy and analyzed by Leica software and Image J.

765

766 **Quantification of fluorescence and statistical analysis**

767 For lacZ/ β -gal intensity analysis, including *EcRE-lacZ*, *Puc-lacZ* and *β Ftz-f1-lacZ*,

768 fluorescence intensity of border cell was measured by Image J and normalized to the
769 nurse cells' staining background to obtain the relative intensity. Statistical analysis
770 was performed with GraphPad Prism 6 using unpaired two-tailed Student's t-test,
771 significance of $p < 0.05$ was used as the criterion for statistical significance and
772 indicated with *, $p < 0.01$ was indicated with **, $p < 0.001$ with three stars (***) and
773 $p < 0.0001$ with ****, not significant was indicated with "ns".

774

775 **3-D imaging of border cell cluster**

776 We used 2 coverslips (0.13-0.17mm thick) as bridges to mount egg chambers so that
777 there is ample space in the z-axis to avoid compression of border cell clusters.
778 Individual confocal sections were captured every 0.4 μm for each z-series of border
779 cell cluster. The z-series was then processed by Imaris software to view 3-D
780 distributions of aPKC, Lifeact-GFP, Par6-GFP and PIP2-GFP (Figure 3, Movies 1-4).

781

782 **Chitin staining**

783 Ovaries were fixed as described for immunostaining but without blocking. FB28
784 (Sigma) was used as a chitin dye as previously reported. We used FB28 (50mg/ml)
785 with dilution of 1:400, stained ovaries in PBST for 30 min, washing 3x10 min with
786 PBST.

787

788

789 **References**

790

791 Akhtar, N., and Streuli, C.H. (2013). An integrin-ILK-microtubule network orients cell polarity
792 and lumen formation in glandular epithelium. *Nature cell biology* *15*, 17-27.

793 Ashburner, M., Richards, G., (1976). Sequential gene activation by ecdysone in polytene
794 chromosomes of *Drosophila melanogaster*. *Dev Biol* *54*.

795 Bai, J., Uehara, Y., and Montell, D.J. (2000). Regulation of invasive cell behavior by taiman, a
796 *Drosophila* protein related to AIB1, a steroid receptor coactivator amplified in breast cancer. *Cell*
797 *103*, 1047-1058.

798 Beccari, S., Teixeira, L., and Rorth, P. (2002). The JAK/STAT pathway is required for border cell
799 migration during *Drosophila* oogenesis. *Mechanisms of development* *111*, 115-123.

800 Beckstead, R.B., Lam, G., and Thummel, C.S. (2005). The genomic response to

801 20-hydroxyecdysone at the onset of *Drosophila* metamorphosis. *Genome biology* 6, R99.
802 Brignoni, M., Podesta, E.J., Mele, P., Rodriguez, M.L., Vega-Salas, D.E., and Salas, P.J. (1993).
803 Exocytosis of vacuolar apical compartment (VAC) in Madin-Darby canine kidney epithelial cells:
804 cAMP is involved as second messenger. *Experimental cell research* 205, 171-178.
805 Bryant, D.M., Datta, A., Rodriguez-Fraticelli, A.E., Peranen, J., Martin-Belmonte, F., and Mostov,
806 K.E. (2010). A molecular network for de novo generation of the apical surface and lumen. *Nature*
807 *cell biology* 12, 1035-1045.
808 Bryant, D.M., Roinot, J., Datta, A., Overeem, A.W., Kim, M., Yu, W., Peng, X., Eastburn, D.J.,
809 Ewald, A.J., Werb, Z., *et al.* (2014). A molecular switch for the orientation of epithelial cell
810 polarization. *Developmental cell* 31, 171-187.
811 Buszczak, M., Freeman, M.R., Carlson, J.R., Bender, M., Cooley, L., and Segraves, W.A. (1999).
812 Ecdysone response genes govern egg chamber development during mid-oogenesis in *Drosophila*.
813 *Development* 126, 4581-4589.
814 Caceres, L., Necakov, A.S., Schwartz, C., Kimber, S., Roberts, I.J., and Krause, H.M. (2011).
815 Nitric oxide coordinates metabolism, growth, and development via the nuclear receptor E75.
816 *Genes & development* 25, 1476-1485.
817 Carney, G.E., and Bender, M. (2000). The *Drosophila* ecdysone receptor (EcR) gene is required
818 maternally for normal oogenesis. *Genetics* 154, 1203-1211.
819 Cliffe, A., Doupe, D.P., Sung, H., Lim, I.K., Ong, K.H., Cheng, L., and Yu, W. (2017).
820 Quantitative 3D analysis of complex single border cell behaviors in coordinated collective cell
821 migration. *Nature communications* 8, 14905.
822 Datta, A., Bryant, D.M., and Mostov, K.E. (2011). Molecular regulation of lumen morphogenesis.
823 *Current biology : CB* 21, R126-136.
824 Devine, W.P., Lubarsky, B., Shaw, K., Luschnig, S., Messina, L., and Krasnow, M.A. (2005).
825 Requirement for chitin biosynthesis in epithelial tube morphogenesis. *Proceedings of the National*
826 *Academy of Sciences of the United States of America* 102, 17014-17019.
827 Domanitskaya, E., Anllo, L., and Schupbach, T. (2014). Phantom, a cytochrome P450 enzyme
828 essential for ecdysone biosynthesis, plays a critical role in the control of border cell migration in
829 *Drosophila*. *Developmental biology* 386, 408-418.
830 Ferrari, A., Veligodskiy, A., Berge, U., Lucas, M.S., and Kroschewski, R. (2008). ROCK-mediated
831 contractility, tight junctions and channels contribute to the conversion of a preapical patch into
832 apical surface during isochoric lumen initiation. *Journal of cell science* 121, 3649-3663.
833 Gauhar, Z., Sun, L.V., Hua, S., Mason, C.E., Fuchs, F., Li, T.R., Boutros, M., and White, K.P.
834 (2009). Genomic mapping of binding regions for the Ecdysone receptor protein complex. *Genome*
835 *research* 19, 1006-1013.
836 Geanette T. Lam1, C.J.a.C.S.T. (1997). Coordination of larval and prepupal gene expression by the
837 DHR3 orphan receptor during *Drosophila* metamorphosis. *Development*, 1757-1769.
838 Hackney, J.F., Pucci, C., Naes, E., and Dobens, L. (2007). Ras signaling modulates activity of the
839 ecdysone receptor EcR during cell migration in the *Drosophila* ovary. *Developmental dynamics : an official publication of the American Association of Anatomists* 236, 1213-1226.
840 Horne-Badovinac, S., and Bilder, D. (2005). Mass transit: epithelial morphogenesis in the
841 *Drosophila* egg chamber. *Developmental dynamics : an official publication of the American*
842 *Association of Anatomists* 232, 559-574.
843 Huang, J., Zhou, W., Dong, W., Watson, A.M., and Hong, Y. (2009). From the Cover: Directed,

845 efficient, and versatile modifications of the *Drosophila* genome by genomic engineering.
846 Proceedings of the National Academy of Sciences of the United States of America *106*,
847 8284-8289.

848 Huet, F., Ruiz, C., and Richards, G. (1995). Sequential gene activation by ecdysone in *Drosophila*
849 *melanogaster*: the hierarchical equivalence of early and early late genes. *Development* *121*,
850 1195-1204.

851 Jang, A.C., Chang, Y.C., Bai, J., and Montell, D. (2009). Border-cell migration requires integration
852 of spatial and temporal signals by the BTB protein Abrupt. *Nature cell biology* *11*, 569-579.

853 Jia, Q., Liu, S., Wen, D., Cheng, Y., Bendena, W.G., Wang, J., and Li, S. (2017). Juvenile hormone
854 and 20-hydroxyecdysone coordinately control the developmental timing of matrix
855 metalloproteinase-induced fat body cell dissociation. *The Journal of biological chemistry* *292*,
856 21504-21516.

857 Kageyama, Y., Masuda, S., Hirose, S., and Ueda, H. (1997). Temporal regulation of the
858 mid-prepupal gene FTZ-F1: DHR3 early late gene product is one of the plural positive regulators.
859 *Genes to cells : devoted to molecular & cellular mechanisms* *2*, 559-569.

860 Koelle, M.R., Talbot, W.S., SeGRAves, W.A., Bender, M.T., Cherbas, P., and Hogness, D.S. (1991).
861 The *drosophila* EcR gene encodes an ecdysone receptor, a new member of the steroid receptor
862 superfamily. *Cell* *67*, 59-77.

863 Kozlova, T., and Thummel, C.S. (2003). Essential roles for ecdysone signaling during *Drosophila*
864 mid-embryonic development. *Science* *301*, 1911-1914.

865 Lam, G.T., Jiang, C., and Thummel, C.S. (1997). Coordination of larval and prepupal gene
866 expression by the DHR3 orphan receptor during *Drosophila* metamorphosis. *Development* *124*,
867 1757-1769.

868 Li, K., Tian, L., Guo, Z., Guo, S., Zhang, J., Gu, S.H., Palli, S.R., Cao, Y., and Li, S. (2016).
869 20-Hydroxyecdysone (20E) Primary Response Gene E75 Isoforms Mediate Steroidogenesis
870 Autoregulation and Regulate Developmental Timing in *Bombyx*. *The Journal of biological*
871 *chemistry* *291*, 18163-18175.

872 Li, T.-R., and White, K.P. (2003). Tissue-Specific Gene Expression and Ecdysone-Regulated
873 Genomic Networks in *Drosophila*. *Developmental cell* *5*, 59-72.

874 Llense, F.M.-B., E. (2008). JNK signaling controls border cell cluster integrity and collective cell
875 migration. *Current biology : CB* *18*, 538-544.

876 Luo, J., Zuo, J., Wu, J., Wan, P., Kang, D., Xiang, C., Zhu, H., and Chen, J. (2015). In vivo RNAi
877 screen identifies candidate signaling genes required for collective cell migration in *Drosophila*
878 ovary. *Sci China Life Sci* *58*, 379-389.

879 Ma, X., Huang, J., Yang, L., Yang, Y., Li, W., and Xue, L. (2011). NOPO modulates Egr-induced
880 JNK-independent cell death in *Drosophila*. *Cell Research* *22*, 425.

881 Ma, X., Shao, Y., Zheng, H., Li, M., Li, W., and Xue, L. (2013). Src42A modulates tumor invasion
882 and cell death via Ben/dUev1a-mediated JNK activation in *Drosophila*. *Cell Death & Disease* *4*,
883 e864-e864.

884 Manning, L., Sheth, J., Bridges, S., Saadin, A., Odinammadu, K., Andrew, D., Spencer, S.,
885 Montell, D., and Starz-Gaiano, M. (2017). A hormonal cue promotes timely follicle cell migration
886 by modulating transcription profiles. *Mechanisms of development* *148*, 56-68.

887 Margaret B, S., Thomas J, K., Charles W, W., and Richard B, I. (1989). Ecdysteroid fluctuations in
888 adult *Drosophila melanogaster* caused by elimination of pupal reserves and synthesis by early

889 vitellogenic ovarian follicles. *Insect Biochemistry* *19*, 243–249.

890 Melani, M., Simpson, K.J., Brugge, J.S., and Montell, D. (2008). Regulation of cell adhesion and
891 collective cell migration by hindsight and its human homolog RREB1. *Current biology : CB* *18*,
892 532-537.

893 Montell, D.J. (2003). Border-cell migration: the race is on. *Nature reviews Molecular cell biology*
894 *4*, 13-24.

895 Montell, D.J., Rorth, P., and Spradling, A.C. (1992). slow border cells, a locus required for a
896 developmentally regulated cell migration during oogenesis, encodes *Drosophila* C/EBP. *Cell* *71*,
897 51-62.

898 Moussian, B., Schwarz, H., Bartoszewski, S., and Nusslein-Volhard, C. (2005). Involvement of
899 chitin in exoskeleton morphogenesis in *Drosophila melanogaster*. *Journal of morphology* *264*,
900 117-130.

901 Moussian, B., Tang, E., Tønning, A., Helms, S., Schwarz, H., Nusslein-Volhard, C., and Uv, A.E.
902 (2006). *Drosophila* Knickkopf and Retroactive are needed for epithelial tube growth and cuticle
903 differentiation through their specific requirement for chitin filament organization. *Development*
904 *133*, 163-171.

905 Ninov, N., Menezes-Cabral, S., Prat-Rojo, C., Manjón, C., Weiss, A., Pyrowolakis, G., Affolter,
906 M., Martín-Blanco, E (2010). Dpp signaling directs cell motility and invasiveness during epithelial
907 morphogenesis. *Curr Biol* *20*, 513--520.

908 Rabinovich, D., Yaniv, S.P., Alyagor, I., and Schuldiner, O. (2016). Nitric Oxide as a Switching
909 Mechanism between Axon Degeneration and Regrowth during Developmental Remodeling. *Cell*
910 *164*, 170-182.

911 Reinking, J., Lam, M.M., Pardee, K., Sampson, H.M., Liu, S., Yang, P., Williams, S., White, W.,
912 Lajoie, G., Edwards, A., *et al.* (2005). The *Drosophila* nuclear receptor E75 contains heme and is
913 gas responsive. *Cell* *122*, 195-207.

914 Richards, G.W.R.A. (1995). Sequential gene activation by ecdysone in *Drosophila melanogaster*:
915 the hierarchical equivalence of early and early late genes. *Development* *121*, 1195-1204

916 Rougvie, A. (2001). Control of developmental timing in animals. *Nature Reviews Genetics* *2*,
917 690–701.

918 Ruaud, A.F., Lam, G., and Thummel, C.S. (2010). The *Drosophila* nuclear receptors DHR3 and
919 betaFTZ-F1 control overlapping developmental responses in late embryos. *Development* *137*,
920 123-131.

921 Sap, K.A., Bezstarosti, K., Dekkers, D.H.W., van den Hout, M., van Ijcken, W., Rijkers, E., and
922 Demmers, J.A.A. (2015). Global quantitative proteomics reveals novel factors in the ecdysone
923 signaling pathway in *Drosophila melanogaster*. *Proteomics* *15*, 725-738.

924 Sigurbjornsdottir, S., Mathew, R., and Leptin, M. (2014). Molecular mechanisms of de novo
925 lumen formation. *Nature reviews Molecular cell biology* *15*, 665-676.

926 Silver, D.L., Geisbrecht, E.R., and Montell, D.J. (2005). Requirement for JAK/STAT signaling
927 throughout border cell migration in *Drosophila*. *Development* *132*, 3483-3492.

928 Strilic, B., Eglinger, J., Krieg, M., Zeeb, M., Axnick, J., Babal, P., Muller, D.J., and Lammert, E.
929 (2010). Electrostatic cell-surface repulsion initiates lumen formation in developing blood vessels.
930 *Current biology : CB* *20*, 2003-2009.

931 Sullivan, A.A., and Thummel, C.S. (2003). Temporal profiles of nuclear receptor gene expression
932 reveal coordinate transcriptional responses during *Drosophila* development. *Molecular*

933 endocrinology *17*, 2125-2137.

934 Terashima, J., and Bownes, M. (2006). E75A and E75B have opposite effects on the
935 apoptosis/development choice of the *Drosophila* egg chamber. *Cell death and differentiation* *13*,
936 454-464.

937 Thummel, C.S. (2001). Molecular mechanisms of developmental timing in *C. elegans* and
938 *Drosophila*. *Developmental cell* *1* 453-465.

939 Tseng, C.Y., Kao, S.H., Wan, C.L., Cho, Y., Tung, S.Y., Hsu, H.J. . (2014). Notch signaling
940 mediates the age-associated decrease in adhesion of germline stem cells to the niche. *PLoS*
941 *genetics*.

942 Vega-Salas, D.E., Salas, P.J., and Rodriguez-Boulan, E. (1988). Exocytosis of vacuolar apical
943 compartment (VAC): a cell-cell contact controlled mechanism for the establishment of the apical
944 plasma membrane domain in epithelial cells. *The Journal of cell biology* *107*, 1717-1728.

945 Wang, S., Jayaram, S.A., Hemphala, J., Senti, K.A., Tsarouhas, V., Jin, H., and Samakovlis, C.
946 (2006). Septate-junction-dependent luminal deposition of chitin deacetylases restricts tube
947 elongation in the *Drosophila* trachea. *Current biology : CB* *16*, 180-185.

948 Wang, X., Adam, J.C., and Montell, D. (2007). Spatially localized Kuzbanian required for specific
949 activation of Notch during border cell migration. *Developmental biology* *301*, 532-540.

950 Webb, A.B., and Oates, A.C. (2016). Timing by rhythms: Daily clocks and developmental rulers.
951 *Development, growth & differentiation* *58*, 43-58.

952 White, K.P., Hurban, P., Watanabe, T., and Hogness, D.S. (1997). Coordination of *Drosophila*
953 metamorphosis by two ecdysone-induced nuclear receptors. *Science* *276*, 114-117.

954 Xiong, G., Wang, C., Evers, B.M., Zhou, B.P., and Xu, R. (2012). RORalpha suppresses breast
955 tumor invasion by inducing SEMA3F expression. *Cancer Res* *72*, 1728-1739.

956 Xiong, G., and Xu, R. (2014). RORalpha binds to E2F1 to inhibit cell proliferation and regulate
957 mammary gland branching morphogenesis. *Molecular and cellular biology* *34*, 3066-3075.

958 Yamanaka, N., Rewitz, K.F., and O'Connor, M.B. (2013). Ecdysone control of developmental
959 transitions: lessons from *Drosophila* research. *Annual review of entomology* *58*, 497-516.

960 Yang, Z., Zimmerman, S., Brakeman, P.R., Beaudoin, G.M., 3rd, Reichardt, L.F., and Marciano,
961 D.K. (2013). De novo lumen formation and elongation in the developing nephron: a central role
962 for afadin in apical polarity. *Development* *140*, 1774-1784.

963 Zhu, K.Y., Merzendorfer, H., Zhang, W., Zhang, J., and Muthukrishnan, S. (2016). Biosynthesis,
964 Turnover, and Functions of Chitin in Insects. *Annual review of entomology* *61*, 177-196.

965

966